10

# New Identity of the Kimberlite Melt: Constraints from Unaltered Diamondiferous Udachnaya – East Pipe Kimberlite, Russia

Vadim S. Kamenetsky, Maya B. Kamenetsky and Roland Maas
*University of Tasmania,*
*University of Melbourne,*
*Australia*

## 1. Introduction

Kimberlite magmas are in many aspects unusual compared to other terrestrial magmatic liquids. They are very rare and occur in small volumes, but their intimate relationships with diamonds make them invaluable to the scientific and exploration communities. The association of kimberlite rocks with diamonds and deep-seated mantle xenoliths links the origin of parental kimberlite magmas to the highest known depths (> 150 km) of magma derivation (e.g. Dawson, 1980; Eggler, 1989; Girnis & Ryabchikov, 2005; Mitchell, 1986; Mitchell, 1995; Pasteris, 1984). Kimberlite magmas would have one of the lowest viscosities and highest buoyancies that enable exceptionally rapid transport from the source region (Canil & Fedortchouk, 1999; Eggler, 1989; Haggerty, 1999; Kelley & Wartho, 2000; Sparks et al., 2006) and preservation of diamonds.

Despite significant research efforts, there is still uncertainty about the true chemical identity of kimberlite parental melts and their derivates. Kimberlite magmas are always contaminated by large quantities of lithic fragments and crystals, unrelated to the evolution of the parental melt. In most cases kimberlites are severely modified by syn- and post-magmatic changes that have altered the original alkali and volatile element abundances. These problems are reflected in the definition of the kimberlite rock as "*both a contaminated and altered sample of its parent melt*" (Pasteris, 1984). Numerous other definitions of the kimberlite commonly reflect on ultramafic compositions and enrichment in volatiles ($CO_2$ and $H_2O$; Clement et al., 1984; Kjarsgaard et al., 2009; Kopylova et al., 2007; Mitchell, 1986; Mitchell, 2008; Patterson et al., 2009; Skinner & Clement, 1979) which are supposedly inherited from parental magmas.

The physical properties of a kimberlite magma directly, and occurrence of diamonds indirectly, relate to the enrichment in carbonate components which are represented in common kimberlites by calcite and dolomite. The abundant carbonate component in kimberlite rocks is counter-balanced by a more abundant olivine (ultramafic) component, represented by olivine fragments and crystals that are commonly affected by serpentinisation. The ultramafic silicate compositions of kimberlites are ascribed to

abundant olivine macrocrysts and phenocrysts, whereas significant $CO_2$ and $H_2O$ contents are attributed respectively to carbonate minerals (calcite and dolomite) and serpentine (+ other $H_2O$-bearing magnesian silicates). Unfortunately, the masking effects of deuteric and post-magmatic alteration do not permit routine recognition of olivine generations, and so the olivine component originally dissolved in the kimberlite parental melt remains controversial (Brett et al., 2009; Francis & Patterson, 2009; Mitchell & Tappe, 2010; Patterson et al., 2009). Similarly, the original magmatic abundances of volatile and fluid-mobile alkali elements are disturbed by syn- and post-emplacement modifications, thus complicating complicating quantification of the parental melt composition if inferred from bulk kimberlite analyses.

The existing dogma about correspondence between compositions of whole rock kimberlites and their parental melt has been recently challenged by the newcomers to the kimberlite scientific community (e.g., Kamenetsky et al., 2004; Kamenetsky et al., 2007a; Kamenetsky et al., 2007b; Kamenetsky et al., 2008; Kamenetsky et al., 2009a; Kamenetsky et al., 2009b; Kamenetsky et al., 2009c; Maas et al., 2005). A breakthrough into understanding of the kimberlite magma chemical and physical characteristics was made possible by detailed studies of the diamondiferous Udachnaya-East kimberlite pipe in Siberia. Unlike other kimberlites worldwide, severely modified by syn- and post-magmatic changes, the Udachnaya-East kimberlite is the only known fresh rock of this type, and thus it is invaluable source of information on the composition and temperature of primary melt, its mantle source, rheological properties of ascending kimberlite magma. This kimberlite preserved unequivocal evidence for olivine populations, olivine paragenetic assemblages and olivine-hosted melt inclusions, and the role of mantle-derived alkali carbonate and alkali chloride components in the parental melt.

## 2. Udachnaya-East kimberlite: Location and samples

The Udachnaya diamondiferous kimberlite pipe is located in the Daldyn-Alakit region of the Siberian diamondiferous kimberlite province (Fig. 1). Most Siberian pipes are tuff-breccias essentially devoid of unaltered olivine, but some contain large blocks of massive fresh kimberlite. A remarkable characteristic of this region is that it contains more pipes with fresh, unaltered olivine than any other kimberlite region within the Siberian province. About 10% of the intrusions exhibit either two adjacent channelways or repeated intrusion of magma through the same chimney. The Udachnaya pipe, the best known example of these twin diatremes, is located in the northwest part of the Daldyn field (Fig. 1). At the surface it consists of two adjacent bodies (East and West) that are separated at depth >250-270 m. Based on stratigraphic relationships both intrusions formed at the Devonian-Carboniferous boundary (~350 Ma), and the age estimates vary from 389 to 335 Ma (Burgess et al., 1992; Kamenetsky et al., 2009c; Kinny et al., 1997; Maas et al., 2005; Maslovskaja et al., 1983). The eastern and western bodies of the Udachnaya kimberlite pipe are different from each other in terms of mineralogy, petrography, composition, and degree of alteration. As the alteration of the western pipe can be considered typical of this rock type, the rocks of the Udachnaya-East are unique in having lesser alteration, and in some places they are completely unaltered.

At depths greater than 350 m a particularly fresh porphyritic kimberlite has been found. These rocks are described as dark-grey massive kimberlite, characterized by unaltered euhedral-subhedral olivine phenocrysts set in a dominantly carbonate matrix (Marshintsev

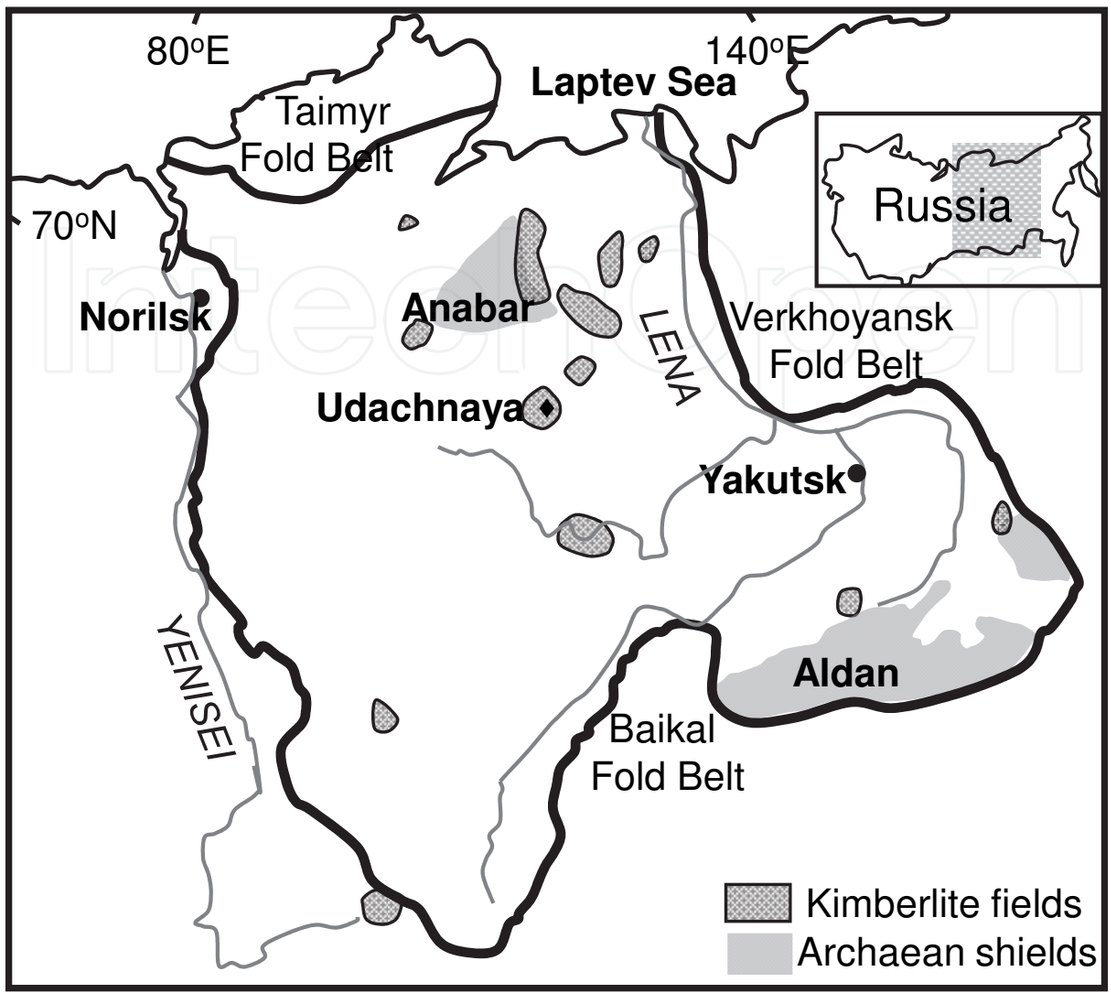


Fig. 1. Map of the Siberian Platform showing the major kimberlite fields after Pearson et al. (1995).

et al., 1976). At deeper levels (> 400 m) of the kimberlite body the amount of serpentine in the groundmass gradually decreases and the amount of carbonate in the groundmass increases. Intensive mining of the Udachnaya pipe revealed widespread chloride minerals (mostly halite) as dispersed masses in the groundmass and massive multi-mineral segregations of halite, serpentine, anhydrite, carbonates and hydrous iron oxides (Pavlov & Ilupin, 1973). The amount of chloride minerals in the groundmass increases with depth, and recently a large number of chloride-carbonate "nodules" were recovered from ~470-500 m depths of the mine.

The studies Udachnaya-East kimberlites are dark massive rocks with porphyroclastic fragmental textures. They are exceptionally olivine-rich (Fig. 2, 12a), a feature shared by the majority of known kimberlites, excluding rare aphanitic kimberlites, such as those from Kimberley, South Africa (Edgar et al., 1988; Edgar & Charbonneau, 1993; le Roex et al., 2003; Shee, 1986) and Jericho, Canada (Price et al., 2000). The large abundance of olivine (45-60 vol%) is reflected in the high MgO content of the bulk rock compositions (28-36 wt%). Olivine is set in a fine-grained matrix of carbonates (Fig. 2, calcite, shortite $Na_2Ca_2(CO_3)_3$ and

zemkorite (Na, K)$_2$Ca(CO$_3$)$_2$), chlorides (halite and sylvite), and minor phlogopite and opaque minerals (e.g. spinel group minerals, perovskite, Fe±(Ni,Cu,K) sulphides) (Golovin et al., 2007; Golovin et al., 2003; Kamenetsky et al., 2004; Kamenetsky et al., 2007a; Sharygin et al., 2003; Sobolev et al., 1989). Groundmass olivine is very abundant (up to 40 vol%), completely unaltered, and contains crystal, fluid and melt inclusions (Fig. 3; Golovin et al., 2003; Kamenetsky et al., 2004; Kamenetsky et al., 2007a; Kamenetsky et al., 2008; Kamenetsky et al., 2009a).

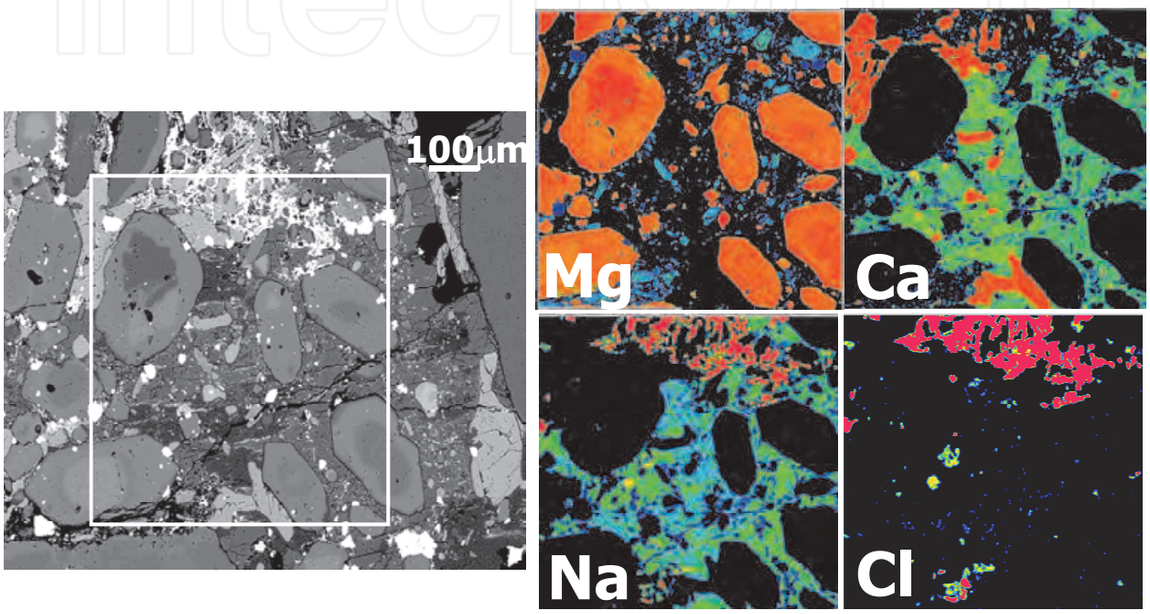


Fig. 2. Backscattered electron image and X-ray element maps showing intimate association of euhedral zoned olivine, Na–K chlorides, alkali carbonates, calcite, and sodalite in the groundmass of Udachnaya-East kimberlite

The bulk rock compositions are also characterised by low $Al_2O_3$ (1.2-2.3 wt%), but high CaO (8.4-18.2 wt%) and $CO_2$ (4-14 wt%) contents. Trace element compositions are similar to those of other kimberlites, having incompatible element enrichment and depletion in heavy rare-earth elements and Y (Fig. 4). The radiogenic isotope data ($^{87}Sr/^{86}Sr_t \approx 0.7047$, $\varepsilon Nd \approx +4$, $^{206}Pb/^{204}Pb_t \approx 18.7$, $^{207}Pb/^{204}Pb_t = 15.53$, $^{208}Pb/^{204}Pb_t = 35.5–38.9$, t = 367 Ma; Maas et al., 2005) fall within the field defined by most group-I kimberlites (Fraser et al., 1985; Smith, 1983; Weis & Demaiffe, 1985). The overall petrographic, mineralogical and chemical characteristics of the Udachnaya-East kimberlites suggest that they are common type-I (Mitchell, 1989) or group-I (Clement & Skinner, 1985; Smith, 1983) kimberlite.

However, the studied Udachnaya-East samples are distinctly different from other kimberlites in that they have high abundances of alkali elements (up to 6 wt% $Na_2O$), strong enrichment in chlorine (up to 6 wt%), and extraordinary depletion in $H_2O$ (< 0.5 wt%) correlated with absence of primary or secondary serpentine. Thus unusual for kimberlites low $H_2O$ abundances coupled with extraordinary enrichment in $Na_2O$ and Cl (Fig. 5) may

indicate that two of the inferred key characteristics of kimberlitic magmas - low sodium and high water contents (Fig. 5; Kjarsgaard et al., 2009) – unambiguously relate to postmagmatic alteration that affected most kimberlites worldwide.

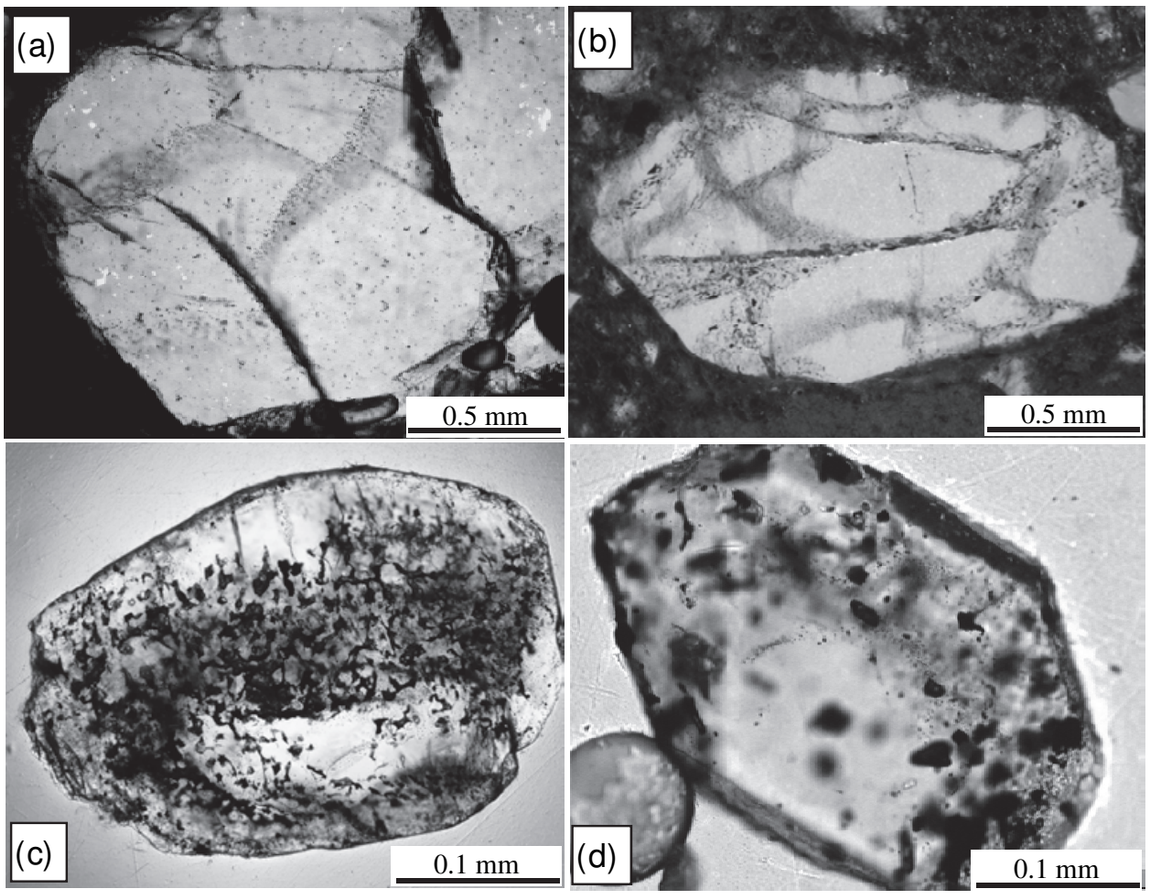


Fig. 3. Photomicrographs in plane-polarised light of individual crystals of olivine-I (a, b) and olivine-II (c, d) showing networks of magmatic inclusions, including crystal, fluid and carbonate-chloride melt inclusions.

## 3. Kimberlite olivine: Morphology and composition

Two populations of olivine in the Udachnaya-East kimberlite can be recognised based on size, colour, morphology, and entrapped inclusions. Consistent with many other studies of kimberlitic olivine (e.g., Boyd & Clement, 1977; Emeleus & Andrews, 1975; Hunter & Taylor, 1984; Mitchell, 1973; Mitchell, 1978; Nielsen & Jensen, 2005; Sobolev et al., 1989) the populations are represented by olivine-I (interpreted by different workers as cognate phenocrysts or xenocrysts) and groundmass olivine-II. However, as it follows from Arndt et al. (2010), Brett et al. (2009) and Kamenetsky et al. (2008) both populations significantly overlap in terms of composition, and possibly origin.

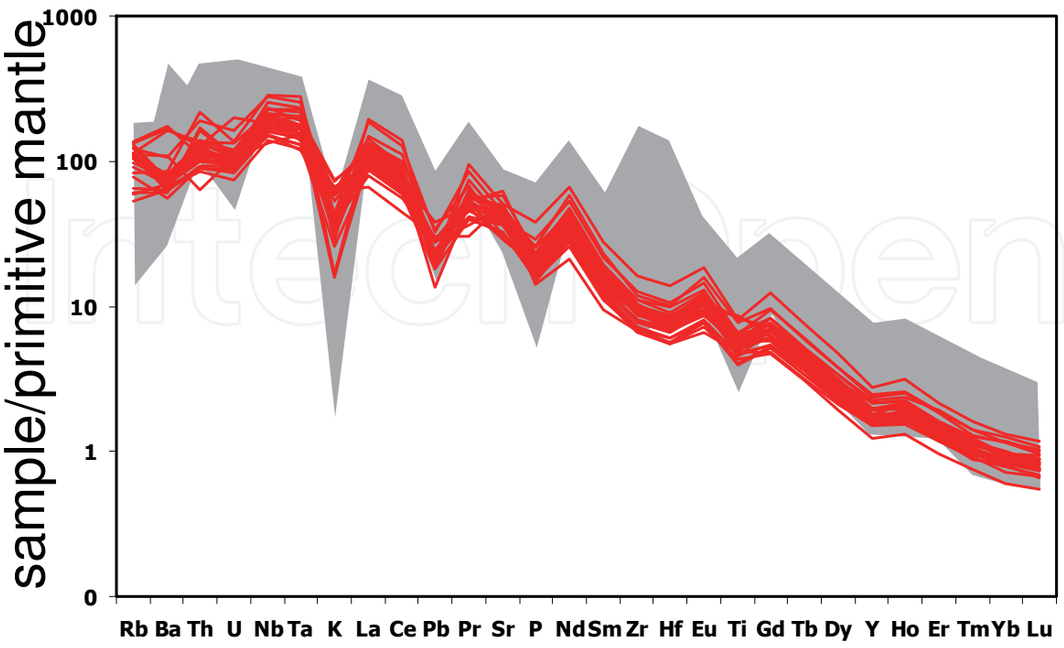


Fig. 4. Trace element abundance patterns of the Udachnaya-East kimberlites (lines) and kimberlites worldwide (field). All compositions are normalised to the "Primitive Mantle" composition of Sun and McDonough (1989).

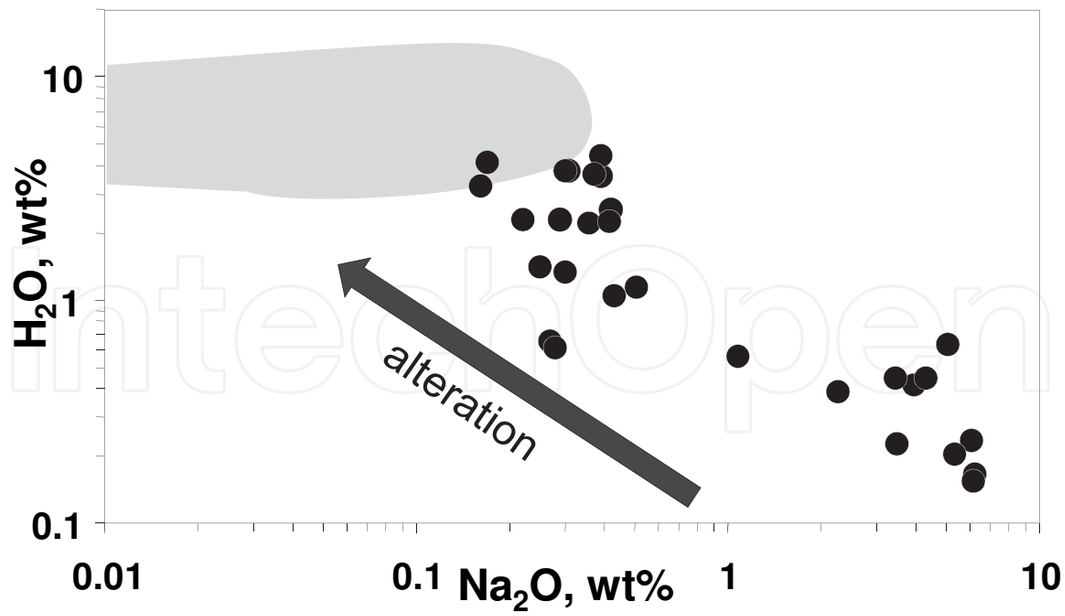


Fig. 5. Compositional co-variations of $Na_2O$ and $H_2O$ (in wt.%) in the Udachnaya-East kimberlites and "archetypal" rocks from South Africa, Greenland and Canada (field). The trend to low sodium and high water contents is considered to be caused by post-magmatic alteration.

### 3.1 Olivine-I

Light-green or light-yellow olivine-I is present as rounded and oval crystals, or more often as angular fragments with smooth edges Fig. 3a, b). Angular olivine-I is characteristically transparent and large (0.5 to 7-8 mm), whereas ovoid grains are smaller (0.7-2 mm) and often 'dusted' with inclusions (Fig. 3a, b). Melt and fluid inclusions occur in angular olivine-I and some round crystals only in "secondary" trails along healed fractures (Fig. 3a, b).
Olivine-I is characterised by variable forsterite content (Fo) from 85 to 94 mol%, although most grains are Fo>91 (Fig. 6a). Most grains appear to be homogeneous, at least in terms of their Fo content, except outermost rims and around healed fractures. Abundances of trace elements Ca, Ni, Cr and Mn in olivine-I vary strongly with Fo (Fig. 6a). The trace element composition trends resembling fractionation can be seen for NiO decreasing (0.43-0.13 wt%) and MnO increasing (0.07-0.17 wt%) as the Fo value decreases (Fig. 6a). However, it should be noted that NiO in the majority of olivine-I is almost constant (0.35-0.39 wt%).

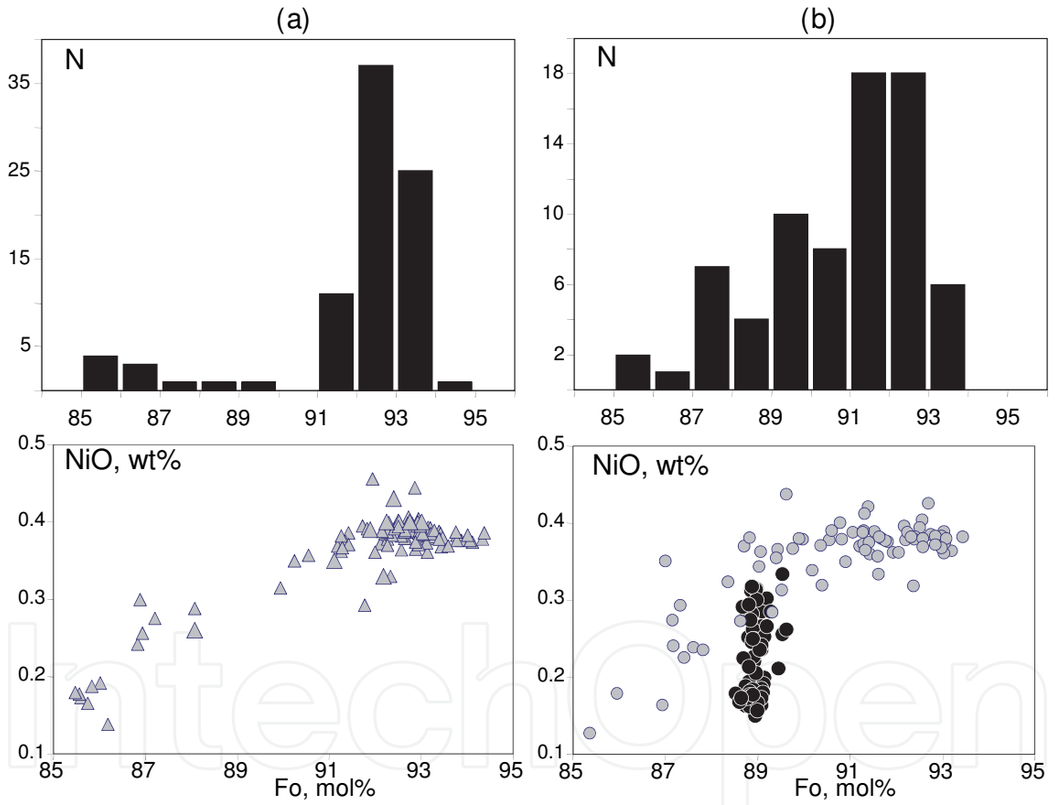


Fig. 6. Forsterite and trace element compositions of olivine-I (a) and olivine-II, 0.3-0.5mm size (b). Grey and black circles represent cores and rims of olivine-II, respectively. N, number of grains. The analytical error (1σ, equals 0.08% for Fo and 2% for NiO) is smaller than the size of the symbols.

### 3.2 Olivine-II: Morphology and zoning

Olivine-II is represented by relatively small (0.05-0.8 mm) euhedral flattened grains (Fig. 3c,d). Crystals display a tabular habit (tablet shape), and crystal growth was preferentially developed in the {100} and {001} directions. Olivine-II is colourless or slightly greenish or

brownish, and a large amount of various inclusions is responsible for weak transparency and "cloudy" appearance of their host crystals (Fig. 3c, d).

The BSE images of individual olivine-II grains demonstrate compositional variability in terms of Fe-Mg relationships (higher and lower Fo correspond to *darker* and *lighter* areas, respectively; Fig. 7). Nearly all groundmass olivine crystals, even the smallest, exhibit intra-grain compositional variability (Fig. 7). The commonly used term "zoning" is not appropriate in the case of olivine-II, as evident from the description below. Five main types of olivine "structure" account for most typical Fo variations within single grains (Fig. 7):

1. A single core, euhedral-subhedral in shape, that can be more forsteritic (1a) or less forsteritic (1b) than the rim;
2. A single resorbed core of variable shape, size and composition. The composition of resorbed cores can be more forsteritic (2a) or less forsteritic (2b) than the rim;
3. A single core separated from rims by a thin layer of distinct composition;
4. Two or more cores of different shape and composition;
5. No distinct core – the grains are either compositionally uniform or have a mosaic-like structure (Fig. 7i).

All olivine-II show abrupt change to extremely Mg-rich ($Fo_{96}$) compositions at the very edge of the grains (~5-10 μm thick) in contact with matrix carbonate.

The grains with a single core (types 1-3) are the most abundant (~80%); however, a single core of euhedral or subhedral shape (type 1) is very rare (5%). Some cores have almost perfect olivine crystal shapes, and as a rule the crystallographic outlines of inner cores are parallel to the whole grain outlines (Fig. 7 a, d-g). The majority of olivine grains have corroded core edges (Fig. 7 b-d, f, h), and the degree of irregularity varies even within a single core. In other words, some outlines of the core can be straight and parallel to the crystal's outer rims, whereas other boundaries of the same core appear highly diffuse. These are transitional between types 1 and 2, and are more abundant than type 1.

Type 2 grains have a single core of variable size (relatively to grain size) and degree of resorption. The majority of the type 2 crystals tend to have oval to very irregular outlines of cores (Fig. 7 b, c, f). Some cores exhibit linear features (e.g. cracks) along which the olivine composition changes.

Types 1 and 2 are additionally subdivided into subtypes with normal ($Fo_{core}>Fo_{rim}$) and reverse ($Fo_{core}<Fo_{rim}$) "zoning".

Type 3 grains with a single core are characterised by presence of a compositionally distinct layer, separating cores and rims (Fig. 7 a, e, f). These layers are variable in shape, continuity and width. Even within a single grain the "separating" layer shows significant variability in shape, width and composition. The composition of such layers in the grains with reverse "zoning" is always more Fo-rich than the composition of both cores and rims.

The crystals belonging to type 4 with two or three cores are relatively rare (14%), but can be very important for genetic interpretations. Typically type 4 is an intergrowth of two distinct grains, where the cores with different or similar Fo have the shape and orientation similar to those of the grain's edges (Fig. 7g). In grains with two or more cores of different compositions, the cores are usually separated from each other (Fig. 7h), although a few examples are noted where the cores coalesce. In some crystals, the core has layers of different compositions, manifesting a gradual or abrupt zoning pattern across the olivine crystals. These layers frequently demonstrate well defined crystallographic shapes, parallel to outermost rims of olivine grains.

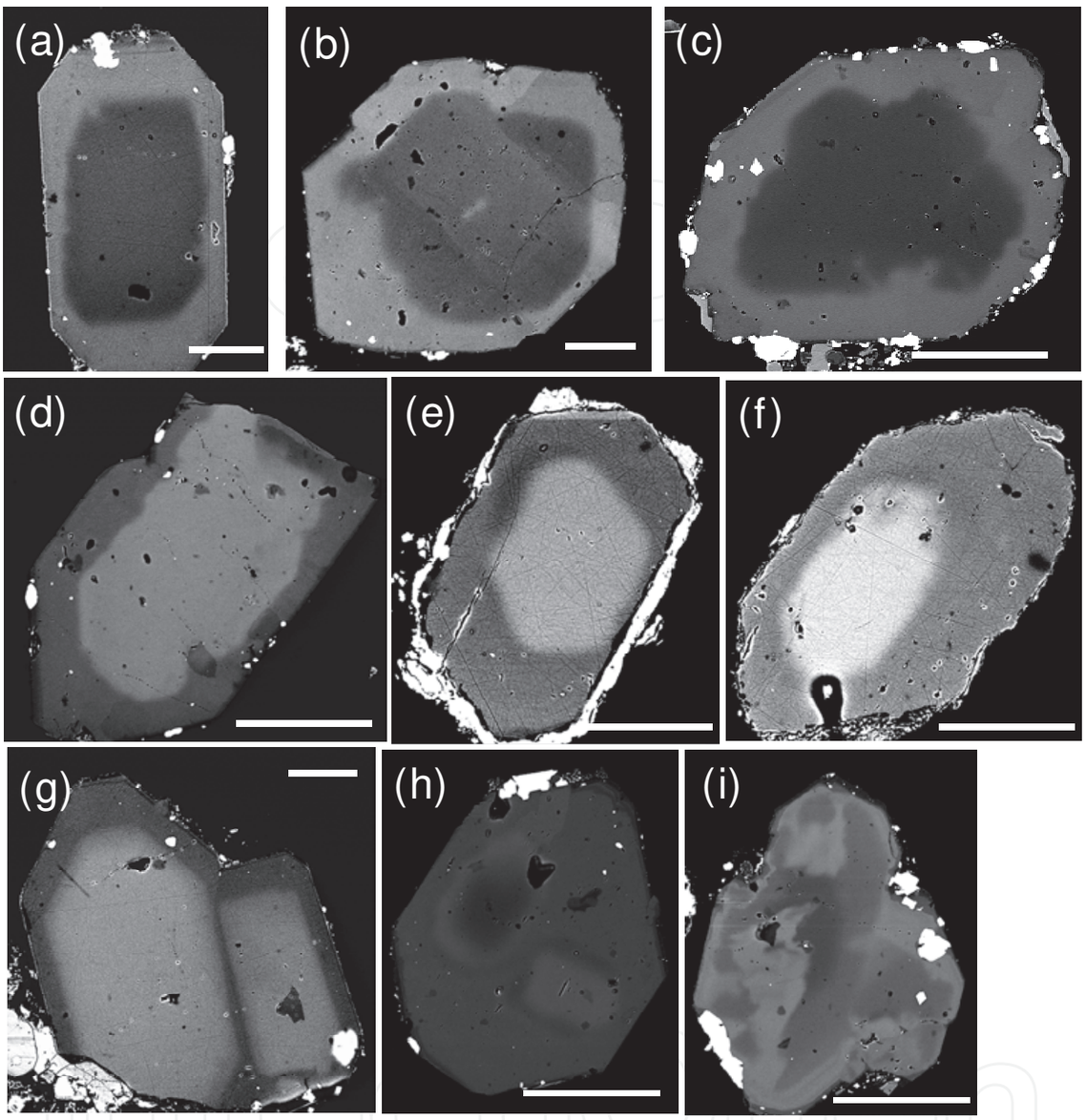


Fig. 7. Back-scattered electron images of olivine-II crystals demonstrating different types of zoning and core and rim relationships. Scale bars represent 100 μm

### 3.3 Olivine-II: Compositional variation

The inner parts ("cores") of olivine-II are strongly variable in Fo content (85.5 - 93.5 mol%), although the compositions 90.5-93 mol% Fo are most common (69%, Fig. 6b). The cores display relatively wide range of NiO (0.13-0.44 wt%, Fig. 6b), CaO (0-0.08 wt%), MnO (0-0.15 wt%), and Cr2O3 (0-0.09 wt%) contents. NiO contents are the highest and almost constant at Fo >89.5, and then gradually decrease in less magnesian olivine (Fig. 6b).

The outer parts ("rims") of olivine-II, although representing significant volumes of this population, have very constant Fo content 89.0 ± 0.2 mol% (Fig. 6b). In contrast, the trace

element abundances in the rims are highly variable (in wt%: NiO 0.15-0.35, CaO 0.03-0.15, MnO 0.11-0.2, $Cr_2O_3$ 0.01-0.11 and $Al_2O_3$ 0-0.04). In general, the rims are richer in MnO, but poorer in NiO than the cores with the same Fo content (Fig. 6b). The outermost forsteritic (Fo96) rims are very enriched in CaO (up to 1 wt%).

## 4. Mineral and melt inclusions in olivine

Inclusions of different composition are present in almost all grains of the Udachnaya-East olivine. They can be very abundant in some grains, but rare in others. Three main types of magmatic inclusions are recognized in the studied samples: crystals, fluid and melt. Inclusion sizes are variable (<1 to ~400 μm) and the distribution of inclusions within a single olivine crystal is very heterogeneous, with some parts totally devoid of inclusions, and some parts so packed with inclusions as to make olivine almost opaque (Fig. 3, 8). The highest density of inclusions is observed along internal fractures and growth planes (Fig. 3). Crystal inclusions in olivine of both populations are always primary. Inclusions of melt and fluid in olivine-I and cores of olivine-II are always restricted to fractures healed with olivine of different composition, and thus are secondary in origin with respect to their host olivine. Similar inclusions in the rims of olivine-II show features reminiscent of both primary and secondary origin (Fig. 8). Melt inclusions in olivine of both populations are predominantly alkali carbonate-chloride in composition (Fig. 8). Silicate melt inclusions have not been found in our studies.

The rims of olivine-II grains contain abundant inclusions of different minerals that are never present in the cores (Kamenetsky et al., 2008; Kamenetsky et al., 2009a). Among them, Cr-spinel, phlogopite, perovskite and rutile are relatively abundant, whereas magnetite and picroilmenite are less common. Inclusions of low-Ca pyroxene (Mg# 88-92) occur in both cores and rims (Fo86-91) in clusters of several (10-30) round and euhedral grains (Kamenetsky et al., 2008; Kamenetsky et al., 2009a). A common association of low-Ca pyroxene in the rims includes numerous melt and fluid inclusions, and $CO_2$-rich bubbles adhered to surfaces of pyroxene crystals. The compositions of low-Ca pyroxene inclusions are characterised by high $SiO_2$ (53.3-58 wt%), $Na_2O$ (0.1-0.9 wt%), elevated $TiO_2$ (0-0.5 wt%), and low $Al_2O_3$ (0.7-1.4 wt%), CaO (0.7-1.7 wt%) and $Cr_2O_3$ (0.1-0.6 wt%), compared to mantle orthopyroxene.

Rare inclusions of high-Ca pyroxene in the Udachnaya-East olivine are restricted to olivine-I and cores of olivine-II (Fig. 9; Kamenetsky et al., 2008; Kamenetsky et al., 2009a). They occur as single crystals or clusters of several crystals. They vary in size (25-400 μm), colour (emerald-green to greyish-green) and shape (round to euhedral-subhedral). Most of them are intimately associated with the carbonate-chloride material, which forms coating on surfaces and inclusions inside clinopyroxene grains (Fig. 9). The clinopyroxene inclusions (Mg# 87.5-94.5 mol%) are in Mg-Fe equilibrium with the host olivine $Fo_{86.3-93}$, and characterised by low $Al_2O_3$ (0.65-2.9 wt%), and high CaO (19.5-23.8 wt%), $Na_2O$ (0.75-2.3 wt%) and $Cr_2O_3$ (0.9-2.6 wt%) contents. Individual crystals show fine-scale compositional zoning, with a general pattern of MgO and CaO increase, and $Na_2O$, $Cr_2O_3$ and in some cases $Al_2O_3$, decrease towards the rims. Major and trace element compositions of high-Ca pyroxene inclusions overlap with compositions of clinopyroxene from lherzolite nodules in the Udachnaya-East kimberlite (Kamenetsky et al., 2009a).

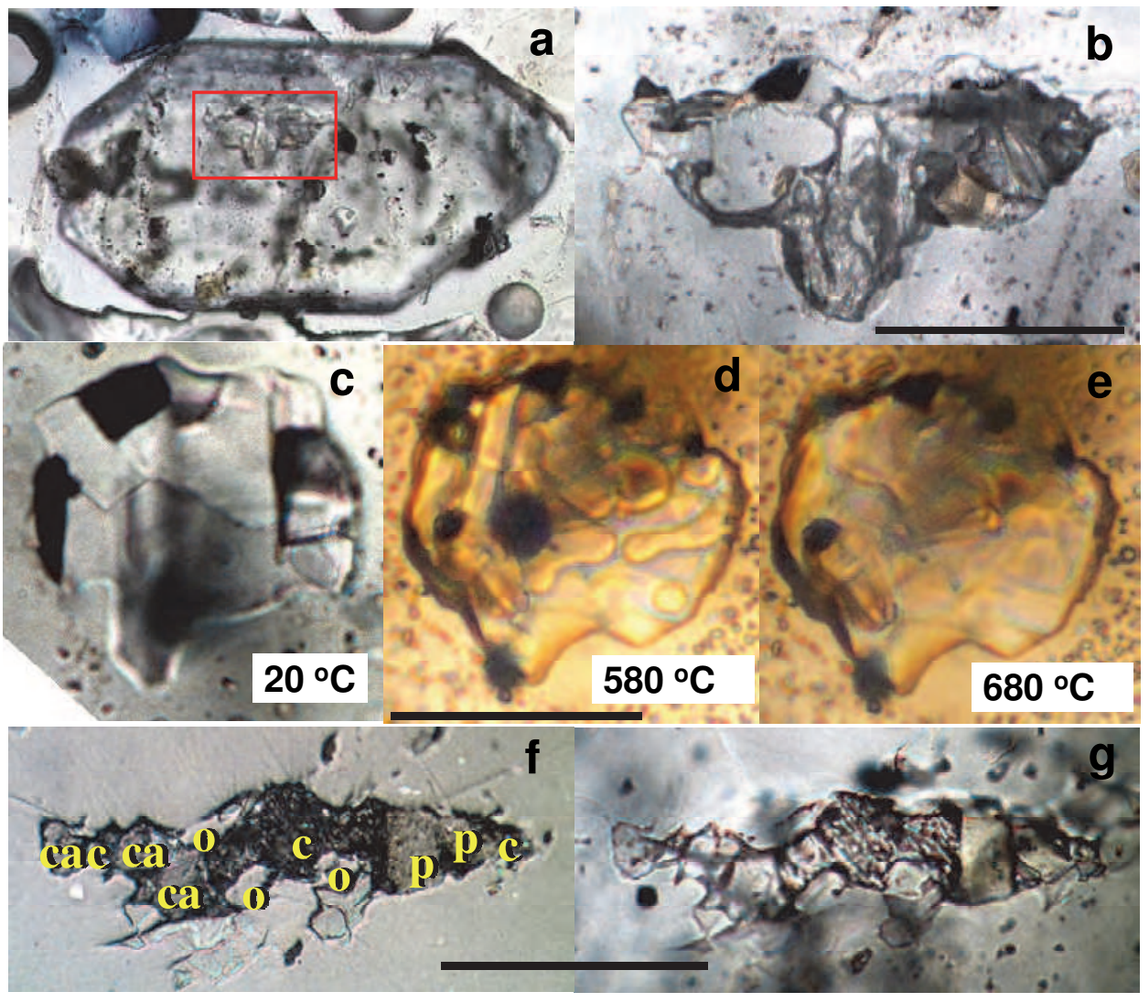


Fig. 8. Photomicrographs of (a) groundmass olivine and (b–g) olivine-hosted melt inclusions. Scale bars represent 50 μm. B: Multiphase melt inclusion hosted in core of olivine (boxed in a). c: Typical melt inclusion at room temperature. d: Same inclusion at 580 °C shows immiscibility between carbonate (matrix) and chloride (globules) melt. e: Same inclusion at 680 °C shows complete miscibility and homogenisation transmitted light). Note sculptured surface of melt inclusion at temperature of homogenisation. f, g: Multiphase melt inclusion in transmitted and reflected light, respectively. Principal daughter phases: c—sodium-potassium chloride; o—olivine; p—phlogopite; ca—sodium-potassium-calcium carbonate

### 4.1 Melt inclusions in groundmass olivine-II

Melt inclusions are trapped either individually within olivine cores and rims, or occur along healed fractures (Fig. 3, 8; Golovin et al., 2003; Kamenetsky et al., 2004; Kamenetsky et al., 2007a). Many inclusions are interconnected by thin channels, and thus modifications of original melt compositions by "necking down" cannot be ruled out. Abundant secondary melt inclusions in fractures connected to the groundmass, and decrepitated inclusions, are assumed to have experienced exchange and loss of material, respectively, after entrapment.

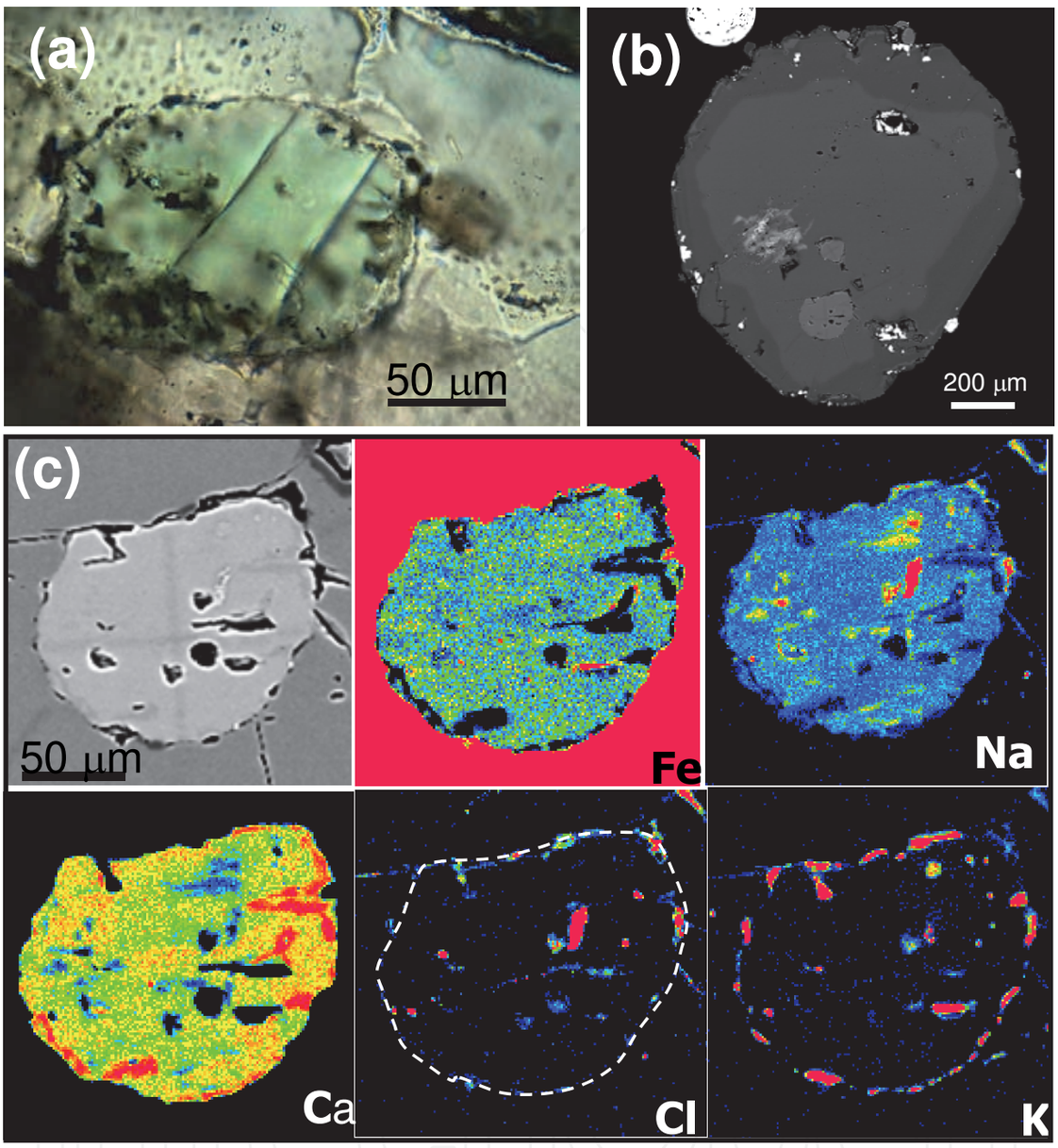


Fig. 9. A plane transmitted light photomicrograph (a) and back-scattered electron image (b) and X-ray element maps (c) of olivine-hosted clinopyroxene inclusions showing carbonate–chloride coatings and melt inclusions associated with clinopyroxene, and fine-scale compositional heterogeneity in terms of Fe, Ca and Na. Clinopyroxene on (c) is a larger inclusion on Fig. 9b. A contour of this inclusion is shown on the Cl Kα map by a dashed line.

"Necking down" can explain variable proportions of fluid and mineral phases in the studied melt inclusions. Fluid components are represented by low-density $CO_2$ bubbles, whereas solid phases are mainly Na-K-Ca carbonates, halite, sylvite, olivine, phlogopite-tetraferriphlopite, calcite, Fe-Ti-Cr oxides, aphthitalite and djerfisherite (Fig. 8f, g; Golovin et al., 2003; Kamenetsky et al., 2004; Sharygin et al., 2003). The inclusions occasionally contain monticellite, humite-clinohumite, northupite, and Ca-Mg-Fe-carbonates.

During heating stage experiments with round, relatively small (40-60 μm) melt inclusions, melting begins at ~160°C, as indicated by jolting movements of either solid phases or vapour bubbles. At 420-580°C bubble movements increase, indicating the appearance of the liquid phase (melt). Daughter phases experience some changes in their relative position, size and shape at 540-600°C. At >600°C we record a number of liquid globules that move freely and change shape continuously (Fig. 8d). The outline of a single globule is always smoothly curved: it can instantaneously change from spherical to cylindrical, embayed or lopsided, similar to an amoeba. With further heating, the number and size of the globules, as well as the number and size of vapour bubbles, gradually decreases. Homogenisation of the inclusions (except some opaque crystals) occurs when the globules and vapour bubbles disappear almost simultaneously (within 20-30°C) at 660-760°C (Fig. 8e).
During slow cooling (5-20°C/min), vapour bubbles nucleate at 690-650°C and then progressively increases in size. Cooling to 610-580°C, the inclusions acquire a 'foggy" appearance for a split second. This process can be best described as the formation of emulsion, i.e, microglobules of liquid in another liquid (melt immiscibility). Microglobules coalesce immediately into elongate or sausage-like pinkish globules. The neighbouring globules ("boudins") are subparallel, and are grouped into regularly aligned formations with a common angle of ~75-80°. A resemblance to a skeletal or spinifex texture is evident for several seconds, after which the original "pinch-and-swell structure" pulls apart giving rise to individual blebs of melt. The latter coalesce and become spherical with time or further cooling. They continue floating, but slow down with decreasing temperature and further coalescence. The exact moment of crystallisation or complete solidification is not detected.

## 5. Chloride-carbonate nodules in kimberlite

The major component of the kimberlite groundmass, carbonate-chloride in composition, sometimes form large segragations ("nodules", Fig. 10; Kamenetsky et al., 2007a; Kamenetsky et al., 2007b). Such samples were collected from fresh kimberlite at the stockpiles of the Udachnaya-East pipe. The assumed depth of their origin in the mine pit is ~500 m. The nodules vary in size from a few cm to 0.5 x 1.5 m, but are commonly 5 to 30 cm across. The shapes are usually round and ellipsoidal, but angular nodules were also encountered. The nodules have very distinct contacts with the host kimberlite, but without any thermometamorphic effects. The contacts are composed of thin (< 1mm) breccia-like aggregate of olivine, calcite, sodalite, phlogopite-tetraferriphlogopite, humite-clinohumite, Fe-Mg carbonates, perovskite, apatite, magnetite, djerfisherite ($K_6(Cu,Fe,Ni)_{25}S_{26}Cl$) and alkali sulphates in a matrix of chlorides. Olivine grains present at the contact with nodules belong to two types: zoned euhedral crystals similar to the Udachnaya-East groundmass olivine-II, and grains with highly irregular shapes and "mosaic" distributions of Fe-Mg.
Based on mineralogy the nodules can be separated into two major groups – chloride (Fig. 10a, b) and chloride-carbonate (Fig. 10 c-e). Chloride minerals are mainly represented by halite with included round grains of sylvite. The grain size, halite colour and transparency are highly variable, ranging from translucent to milky white and from white to all shades of blue. White and blue halite is often randomly interspersed, although in some coarse-grained nodules the interior parts are blue and dark-blue coloured, whereas rims are almost colourless (Fig. 10b). Chloride nodules always contain variable amount of fine-grained

silicate-carbonate material (from 1 to 20 vol%) that is either present interstitially among halite crystals or forms irregular compact masses veined by chlorides. Contacts between silicate-carbonate material and chlorides are decorated by euhedral grains of olivine, monticellite, djerfisherite, perovskite, pyrrhotite, shortite and magnetite.


Fig. 10. Occurrence of chloride nodules in kimberlite (a, b) and textural characteristics and mineral relationships in the chloride–carbonate nodules (c-e). c, d—sample UV-5a-03 show texture resembling liquid immiscibility; white zoned sheets are composed of carbonates (Na–Ca±K±S), greyish masses cementing sheets are chlorides (halite–sylvite). e—sample UV-2-03, composed of shortite, northupite and chlorides. Scale: 1 graticule=1 mm

Chloride-carbonate nodules contain roughly similar amounts of chloride and carbonate minerals that are regularly interspersed (Fig. 10 c-e). Carbonates are present as 1-5 mm thick sheets with a bumpy or boudin-like surface. The groups of aligned, subparallel sheets make up rhombohedron formations (2-2.5 cm) that resemble hollow (skeletal) carbonate crystals (~78° angle) in shape. Cross-sections of inflated parts of the sheets show symmetrical zoning that reflects the change from translucent to milky-white carbonate (Fig. 10 c, d). The intra-sheet space and cracks in carbonate sheets are filled with sugary aggregates of chloride minerals. A texturally and mineralogically different variety of the chloride-carbonate nodules is represented by a single sample UV-2-03 (Fig. 10e). In this ~15 cm nodule, carbonates are present as very thin (< 0.2 mm) aligned white calcite-shortite sheets, as well as individual well-formed yellowish crystals of shortite and northupite (up to 1 cm). In the carbonate intergrowths northupite is interstitial and less abundant (25-30%), and can be distinguished from shortite by crystallographic properties and higher transparency.

### 5.1 Mineralogy of chloride-carbonate nodules

The chloride component of the nodules is dominated by halite, whereas individual grains of sylvite are rare. Typically, sylvite is included in halite, making up to 30 vol% of the chloride assemblage, and in places halite is sprinkled with minute sylvite crystals. Sometimes sylvite inclusions in halite show crystallographic outlines, however, round, lens-shaped and ameboid-like blebs of sylvite with different sizes and orientations are a prominent feature of the chloride masses (Fig. 11). Sylvite domains are often extremely irregular in shape, with curved re-entrances and attenuated swellings. Some domains are thin and elongated, and they can be either subparallel or perpendicular to the contacts with the carbonate sheets (Fig. 11 a-c). Chloride minerals also seal fractures in carbonates (Fig. 11).

The carbonate sheets are very heterogeneous in texture and composition (Figs. 11). In some occurrences a patchy distribution of textures and compositions is observed, but commonly a symmetrical zoning across carbonate sheets exists (Fig. 11b). The Na-Ca carbonate (shortite-like) at the rims, near contacts with chlorides forms intergrowths of acicular crystals. The interstitial space between these crystals (at polished surfaces) is either porous or filled with chlorides and Na-K sulphates. The transition from rims to cores is very distinct (Fig. 11b), as the cores do not show crystalline structure and are principally different in composition. On average the carbonate core is characterised by Na-Ca composition with significant $K_2O$ and $SO_3$. Highly variable, but with good correlation, amounts of $SO_3$ (up to 13 wt%) and $K_2O$ (up to 14 wt%) in the individual analyses of core carbonates suggest that Na-Ca carbonates are intermixed with tiny K-(Na) sulphate phases, the presence of which can be identified at high magnification. The Ca/Na in the core carbonate is higher than in the rim carbonate. Another Na-Ca carbonate with the highest Ca/Na is developed along the cleavage planes in the core and at the contacts with the rims.

An alkali sulphate, aphthitalite $(Na_{0.25}K_{0.75})_2SO_4$, is a minor but widespread component of the carbonate-chloride nodules. It is always associated with halite as irregular blebs, fringing the outmost rims of carbonate sheets (Fig. 11d), and filling fractures and interstitial spaces in carbonates (Fig. 11).

Anhydrous and hydrated Na-Ca carbonates with variable Ca/Na ratios are typical in all nodules, but in one sample (UV-2-03, Fig. 10e) an end-member shortite composition $Na_2Ca_2(CO_3)_3$ was found in close association with Cl-bearing Na-Mg carbonate (northupite – $Na_3Mg(CO_3)_2Cl$). Unlike heterogeneous and thus barely transparent carbonates in other nodules, well-formed crystals of shortite and northupite are clear and can be used for the inclusion studies. The mineral assemblage in this nodule is very complex, and includes euhedral crystals of apatite and phlogopite, as well as tetraferriphlogopite, djerfisherite, K-Na and Na-Ca sulphates, Ba-, Ca- and Sr-Ca-Ba- sulphates and carbonates, calcite, perovskite, and bradleyite $Na_3Mg(PO_4)(CO_3)$. The above minerals are present in aggregates within the interstitial chloride cement and as inclusions in shortite.

Maas et al. (2005) concluded that Sr-Nd-Pb isotopic ratios for the silicate, carbonate and halide components in the groundmass of the Udachnaya-East kimberlite support a mantle origin for the carbonate/chloride components. This conclusion relies in part on accurate age corrections to measured 87Sr/86Sr. However, the extreme instability of magmatic halides and alkali carbonates in air, even on the timescale of hours and days (Zaitsev & Keller, 2006), means that Rb-Sr isotope systematics of these kimberlites may have been modified since kimberlite emplacement in the late Devonian. An attempt to use Cl isotopes as a direct

tracer of chlorine also proved inconclusive because of the similar $^{37}Cl/^{35}Cl$ ratios in mantle and crustal rocks (Sharp et al., 2007).

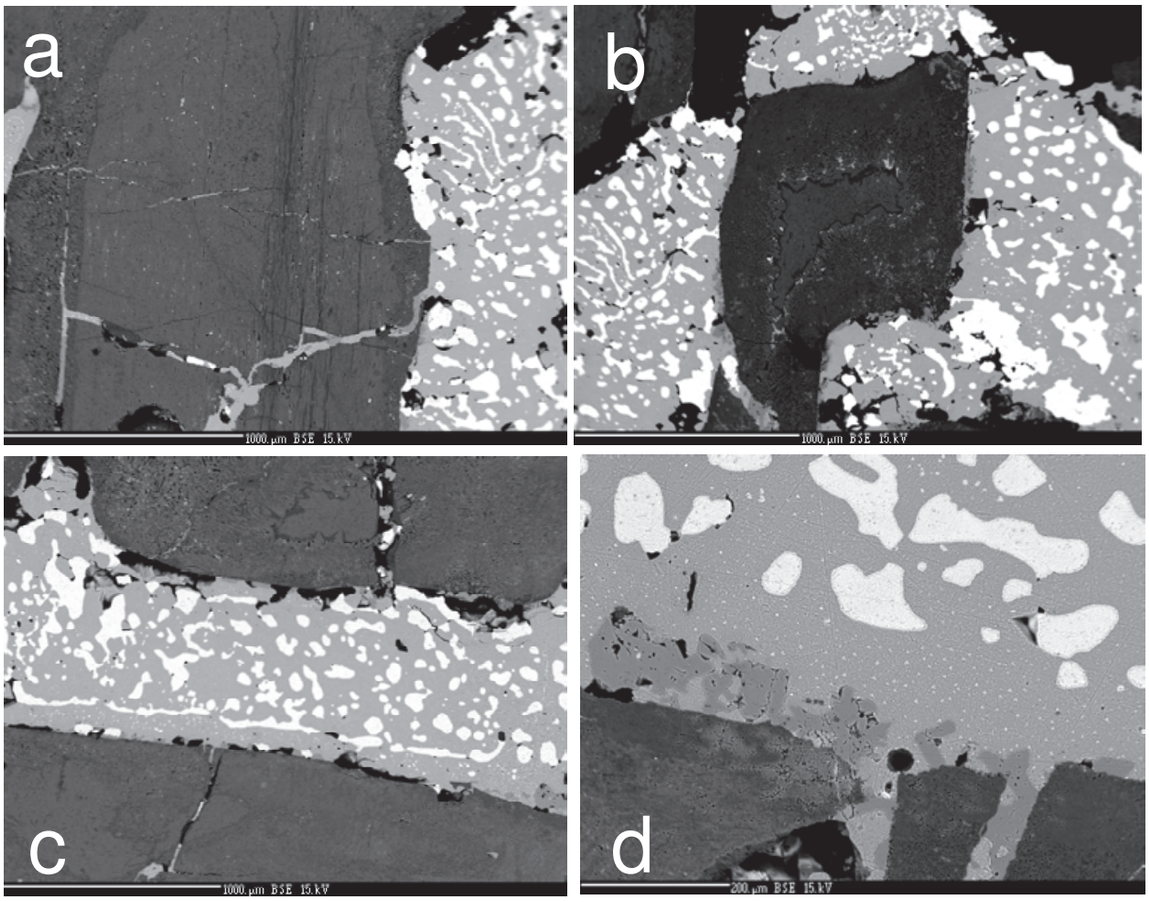


Fig. 11. The nodule texture is determined by a carbonate–chloride grid. Chloride minerals are represented by massive halite (light-grey, hosting amoeboid blebs of sylvite (white). Halite away from large sylvite formations is sprinkled with minute sylvite grains. Often sylvite forms streaks that show distinctive alignment. The overall texture of chloride layers and shape and distribution of sylvite, are reminiscent of liquid immiscibility. Carbonate sheets are symmetrically zoned (a, b). Irregular aphthitalite (grey) is present in halite, always near contacts with carbonate and in veinlets in carbonate (d).

## 6. Radiogenic isotope composition

An alternative approach to tracing relative contribution of mantle and crustal sources to the primary kimberlite melt is based on a study of perovskite, a common late-stage groundmass mineral in kimberlites (Chakhmouradian & Mitchell, 2000). Perovskite ($CaTiO_3$, >1000 ppm Sr, Rb/Sr≈0) should record the $^{87}Sr/^{86}Sr$ of the kimberlite melt at the time of perovskite formation (Heaman, 1989; Paton et al., 2007).

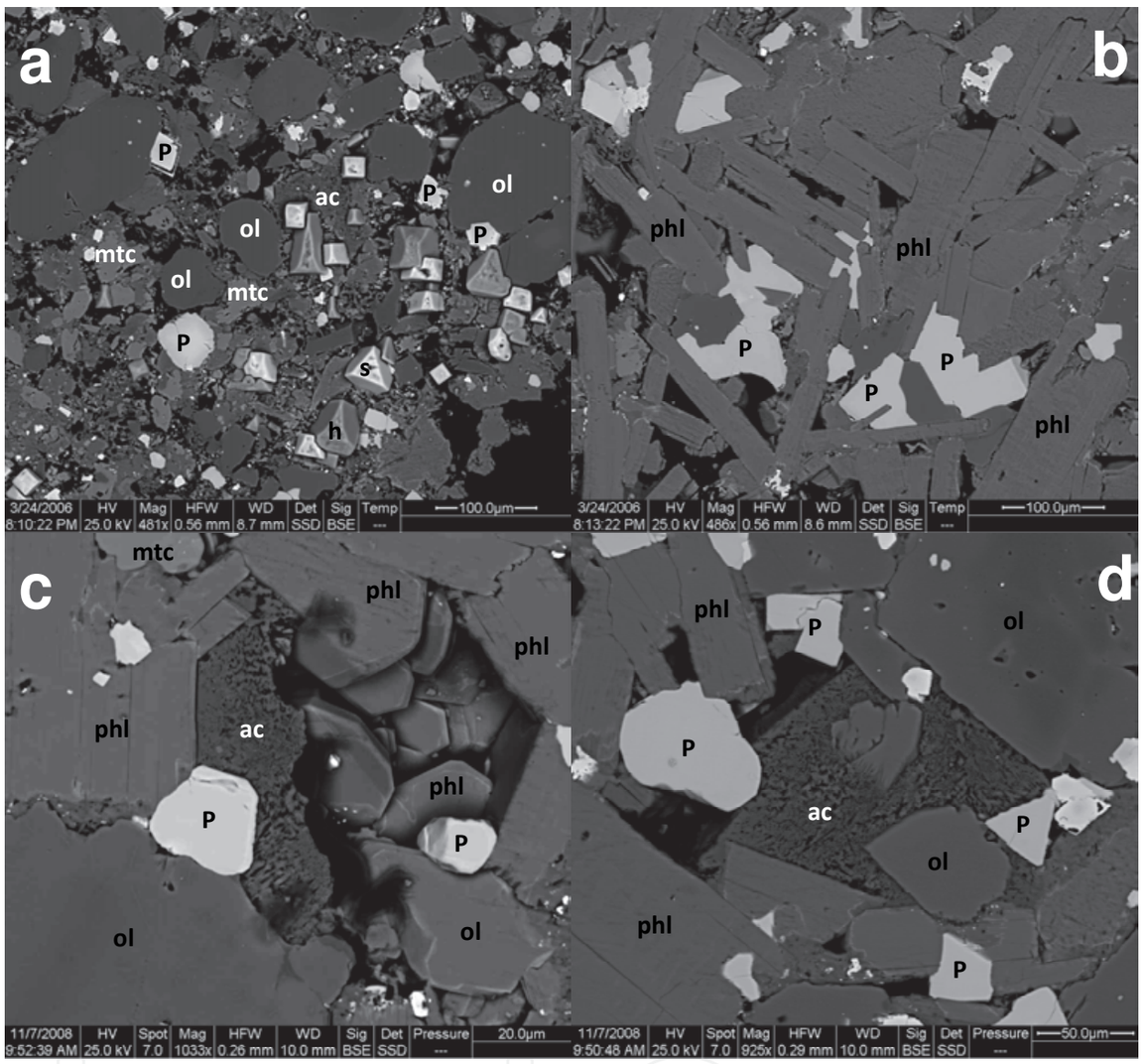


Fig. 12. Backscattered electron images of polished surfaces of the Udachnaya-East kimberlites (a — host kimberlite; b–d — perovskite- and phlogopite-rich clast), showing typical groundmass assemblage of co-crystallised chlorides, halite (h) and sylvite (s), alkali carbonates (ac), perovskite (P), phlogopite (phl), monticellite (mtc) and olivine (ol).

Perovskite is particularly abundant (10%) in sample UV31k-05 (Fig. 12 b-d), an ultramafic (31 wt% MgO), spherical clast ("nucleated autholith" after Mitchell, 1986) found at ~500 m depth in the pipe (Kamenetsky et al., 2009c). Accumulation of perovskite in kimberlite magmas is not unusual and has been reported in other kimberlites (Dawson & Hawthorne, 1973; Mitchell, 1986). The autolith and its host kimberlite are broadly similar in composition, and have the same groundmass assemblage, including interstitial carbonates, chlorides and perovskite (Fig. 2, 12a). Importantly, perovskite is interstitial to phlogopite crystals (Fig. 2b), and thus appears to be later than phlogopite in crystallisation sequence. On the other hand, textural relationships between perovskite and alkali carbonates and chlorides (Fig. 12a, c, d) suggest their co-precipitation from the melt. The melt that crystallised olivine and

phlogopite, the earliest minerals in this assemblage, is recorded in melt inclusions. Phlogopite-hosted melt inclusions in this sample (Kamenetsky et al., 2009c) are identical to olivine-hosted melt inclusions, described in the host kimberlite, in having essentially carbonate-chloride compositions and low homogenisation temperatures (650-700°C).

Three Sr isotope analyses of UV31k-05 perovskite by solution-mode average 0.70305±7 (2σ, age-corrected), similar to laser ablation MC-ICPMS results for 20 individual perovskite grains (average 0.70312±5, 2σ, age-corrected). These $^{87}Sr/^{86}Sr_i$ ratios are lower than those for the host kimberlite (0.7043-0.7049, Kostrovitsky et al., 2007; Maas et al., 2005; Pearson et al., 1995), although results for acid-leached kimberlite (0.7034-0.7037, Maas et al., 2005) provide a closer match. Such offsets between perovskite and host kimberlite were also noticed elsewhere (Paton et al., 2007), and probably reflect minor disturbance of bulk rock Rb-Sr systems. The perovskite-derived Sr isotope ratios are therefore considered a more robust estimate of kimberlite melt $^{87}Sr/^{86}Sr_i$. A ratio of ~0.7031 is the most unradiogenic among bulk rock compositions for group-I archetypal (Nowell et al., 2004; Smith, 1983; Smith et al., 1985) and Siberian kimberlites (Kostrovitsky et al., 2007), and similar to ratios for modern oceanic basalts, including MORB. The Sr isotope data, together with εNd-εHf near +5, are consistent with a parental magma derived from a depleted mantle-like source and suggest an absence of crustal (higher $^{87}Sr/^{86}Sr$, lower εNd) components in the Udachanya-East kimberlite melt, even at the time when perovskite and associated late-stage minerals, including chlorides, crystallised within autolith UV31k-05. This in turn supports a mantle origin of the chlorides in UV31k-05 and similar halides in the host kimberlite.

## 7. Discussion

### 7.1 Major mineral and chemical components of kimberlites

In general, the broad compositional range of kimberlites is defined by two end-members, magnesian silicate (olivine and serpentine) and carbonatitic (calcite). Thus, the kimberlites worldwide form a trend between these two end-members. It is likely that several processes can account for this compositional array. For example, crystallisation of olivine and segregation of carbonatitic melt (Ca increase) is counter-balanced by olivine accumulation and removal of carbonatitic melt (Ca decrease). Whatever the reason for the build-up in Ca, a general consensus exists that the magmatic carbonatitic component is an integral part of all kimberlite rocks, and their parental magmas. What still remains to be understood is why an expected increase in concentrations of alkali elements (Na and K) during the evolution of the kimberlite magmas is not reflected in the compositions of common kimberlites (e.g., $Na_2O$ is invariably <0.3 wt%). Moreover, low abundances of these elements relative to the elements of similar incompatibility are not easily reconciled with expected geochemical characteristics of low-degree mantle melts, even if residual phlogopite is present in the source peridotite (le Roex et al., 2003).

The idea of an alkali element loss and a $H_2O$ gain in kimberlites during post-magmatic processes can be promoted based on the fact that all kimberlites studied to date are inherently altered rocks. The alteration of the carbonate fraction towards essentially alkali-free calcitic compositions has been advocated since the discovery of modern alkali natrocarbonatite lavas from the Oldoinyo Lengai volcano and their altered counterparts (Clarke & Roberts, 1986; Dawson, 1962a; Dawson, 1989; Dawson et al., 1987; Deans & Roberts, 1984; Gittins & McKie, 1980; Hay, 1983). Rapid degradation of alkali carbonates and

dissolution of alkali chlorides in crustal environments (Zaitsev & Keller, 2006) can be responsible for depriving kimberlites (carbonatites) of their original sodium and potassium.

### 7.2 Alkali carbonate-chloride parental melt

The source and origin of alkali carbonates and chlorides in the groundmass of the Udachnaya-East kimberlites is still controversial, given the fact that other group-I kimberlites are devoid of these minerals, but have serpentine. Three possible scenarios of the alkali carbonate-chloride enrichment of the Udachnaya-East rocks can be considered: postmagmatic alteration, contamination of the magma in the crust en route to the surface and derivation from melting of the respectable mantle source. A possibility of post-emplacement ingress of chloride- and carbonate-bearing fluids can be confidently rejected on the basis of petrographic evidence. Any alteration features, typical of kimberlite rocks, are absent in this case; macrocrysts and phenocrysts of olivine bear no serpentine, and the olivine- and phlogopite hosted melt inclusions, trapped at magmatic temperatures (> 660oC) are compositionally similar to the groundmass (Golovin et al., 2007; Golovin et al., 2003; Kamenetsky et al., 2004; Kamenetsky et al., 2007a; Kamenetsky et al., 2009c). Moreover, water-soluble carbonate and chloride minerals in the groundmass were an important factor in preventing ingress of external fluids.

A choice between crustal and mantle origin of the Udachnaya-East unique compositional features is utterly important in deciding whether the Udachnaya-East kimberlite is a "black sheep" in the kimberlite clan or a bearer of the true identity of the primary kimberlite melt, and by inference, the composition of the mantle source and mantle melting process. A potential Na- and Cl-rich contaminant in the form of carbonate–evaporate sedimentary sequence is present in the south and southwest of the Siberian platform, however, it is not confidently recorded in the north, beneath the Daldyn kimberlite field (Brasier & Sukhov, 1998). Moreover, such contaminant is not pronounced in the composition of kimberlites from upper levels of the Udachnaya-East pipe (< 450 m), Udachnaya-West and other pipes from the same field and other kimberlite fields in Siberia. In addition to indirect evidence against likelihood of contamination of the kimberlite magma by evaporites reported in (Kamenetsky et al., 2007a), the deep mantle origin of the carbonate-chloride enrichment of the Udachnaya-East melt is well supported by the isotope composition of Sr in groundmass carbonates and perovskite (Kamenetsky et al., 2009c).

The non-silicate residual kimberlite magma has low temperatures (<650-750oC), as shown by the study of the Udachnaya-East melt inclusions (Kamenetsky et al., 2004), experimental data on the fluorine-bearing Na2CO3-CaCO3 system (Jago & Gittins, 1991) and direct temperature measurements in the halogen-rich (up to 15 wt% F+Cl, Jago & Gittins, 1991) natrocarbonatite lava lakes and flows of the Oldoinyo Lengai volcano (Dawson et al., 1990; Keller & Krafft, 1990; Krafft & Keller, 1989). However, even at these temperatures it is highly fluid. Thus, we envisage that droplets of residual melt separate from a solid aluminosilicate framework of the magma, percolate into weaker, less solidified zones, and finally coalesce, forming melt pockets. The latter are now seen in the kimberlite as chloride-carbonate nodules.

We emphasise that in the Udachnaya-East kimberlite the combination of such features such as extraordinary freshness, high abundances of Na, K and Cl, depletion in H2O, and preservation of water-soluble minerals and chloride-carbonate melt pockets cannot be coincidental. From the analogy with dry carbonatite magmas of Oldoinyo Lengai (Keller &

Krafft, 1990; Keller & Spettel, 1995) and experimental evidence that alkali carbonatite magmas "will persist only if the magma is dry" (Cooper et al., 1975) we conclude that the parental magma of the studied kimberlite was essentially anhydrous and carbonate-rich. This is indirectly supported by the spectroscopic study of micro-inclusions in Udachnaya cubic diamonds that showed that their parental media was a $H_2O$-poor carbonatitic melt (Zedgenizov et al., 2004).

Chlorine and $H_2O$ show opposing solubilities in fluid-saturated silicate melts, as they apparently compete for similar structural positions in the melt. Although Cl does not form complexes with Si in a melt, it may complex with network modifier cations, especially the alkalies, Ca and Mg (Carroll & Webster, 1994). General "dryness" of carbonatites and enrichment of natrocarbonatites in halogens (Gittins, 1989; Jago & Gittins, 1991; Keller & Krafft, 1990) suggest that Cl and $H_2O$ decouple which can be an intrinsic feature of carbonate-rich kimberlite magmas. If this is the case, the conventional role of H2O in governing low temperatures and low viscosities of kimberlite magmas can be readdressed to Cl. Furthermore, the data on carbonate-chloride compositions of melt inclusions in diamonds (Bulanova et al., 1998; Izraeli et al., 2001; Izraeli et al., 2004; Klein-BenDavid et al., 2004), nucleation and growth of diamonds in alkaline carbonate melts (Pal'yanov et al., 2002) and catalytic effect of Cl on the growth of diamonds in the system C–$K_2CO_3$–KCl (Tomlinson et al., 2004) concur with the proposed mantle origin of chloride and alkali carbonate components in the Udachnaya-East kimberlite.

### 7.3 Liquid immiscibility and crystallisation of residual kimberlite magma

Liquid immiscibility is observed in the olivine-hosted melt inclusions at ~600°C on cooling (Fig. 8d). The immiscible liquids are recognized as the carbonate and chloride on the basis that these minerals are dominantly present in the unheated melt inclusions (Golovin et al., 2003; Kamenetsky et al., 2004). Remarkable textures, observed in melt inclusions at the exact moment of melt unmixing (Fig. 8d), is governed by the carbonate crystallographic properties. The presence of similar textures in the chloride-carbonate nodules (Fig. 10 c-e) is the first "snapshot" record of the unambiguous chloride-carbonate melt immiscibility in rocks. The previous natural evidence was based on melt and fluid inclusions in the skarn minerals of Mt Vesuvius (Fulignati et al., 2001) and kimberlitic diamonds (Bulanova et al., 1998; Izraeli et al., 2001; Izraeli et al., 2004; Klein-BenDavid et al., 2004). However, the extensive review of experimental studies (Veksler, 2004) points to the lack of data for chloride–carbonate systems.

Given the analogy with the texture of melt inclusions at the onset of immiscibility, the boudin-like shape of the carbonate sheets and their subparallel alignment (Fig. 10c, e), argues for preservation of primary (instantaneous) immiscibility texture. This means that post-immiscibility (< 600°C) cooling and crystallisation were fast enough to prevent aggregation of one of the immiscible liquids into ovoid or spherical globules that are more typical of steady-state immiscibility. Occurrence of the chloride-rich veinlets in the carbonate sheets (Fig. 11) testifies to later solidification of the chloride liquid relative to carbonate crystallisation. The round and ameboid-like bleb textures of sylvite in halite (Fig. 11) are also reminiscent of liquid immiscibility. In theory this contradicts the fact of complete miscibility in the system NaCl-KCl above the eutectic point of ~660°C. However, the separation of the Na-K chloride melt from the carbonatitic melt, in the case of Udachnaya-East residual melt pockets, occurred at temperatures below the eutectic, and

thus the chloride liquid was supercooled. On the other hand, it was close to the point of solid solution unmixing in the system 75% NaCl – 25% KCl (543$^{o}$C at 1 atm), and in this case unmixing of liquids rather than solids is more likely.

Crystallisation from a homogeneous chloride-carbonate liquid (i.e., prior to immiscibility) is possible, and very unusual Na-Mg carbonates containing a NaCl molecule (northupite $NaCl*Na_2Mg(CO_3)_2$, Fig. 10e), is an example. Disruption of the melt structure caused by chloride-carbonate immiscibility and followed by reduction in solubility of the phosphate and Fe-Mg aluminosilicate components, prompted rapid crystallisation of zoned and often skeletal micro-crystals of apatite and phlogopite - tetraferriphlogopite. Fibrous aggregates of phlogopite in carbonates and sylvite are common and suggestive of incomplete extraction of the phlogopite component from carbonate and chloride melts by post-immiscibility crystallisation. After chloride-carbonate liquid unmixing the sulphate component of the original melt was largely accommodated within the carbonate melt. It was partially released as an aphthitalite melt at the chloride-carbonate interfaces (Fig. 11d), leaving porous K- and S-free carbonate behind (Fig. 11b), and it was also partially exsolved and re-distributed within the carbonate at subsolidus temperatures.

### 7.4 Rheological properties of kimberlite magmas

Kimberlites, especially those with preserved diamonds (Haggerty, 1999) are undoubtedly fast ascending magmas (>4 m/s; see review in Sparks et al., 2006). Support to this contention also comes from experimentally studied rates of dissolution of garnet in $H_2O$-bearing kimberlite melt (Canil & Fedortchouk, 1999) and Ar diffusive loss profiles of phlogopite in mantle xenoliths (Kelley & Wartho, 2000). Other indirect evidence includes inferred low viscosity of the kimberlite magma and its low density, contributing to high buoyancy (Spence & Turcotte, 1990). The unique physical properties of the kimberlite magma are governed by high abundances of chemical components that reduce melt polymerization (e.g. volatiles). The kimberlite magmas are assigned significant $H_2O$ contents in controlling transport and eruption, and only a few studies cast doubts on magmatic origin of $H_2O$ in kimberlites (e.g., Marshintsev, 1986; Sheppard & Dawson, 1975; Sparks et al., 2006).

Rapid transport and emplacement of the Udachnaya-East kimberlite is supported by the fact that this pipe is one of the most diamond-enriched in the world. However, our study denies the control from H2O on rheological properties of the Udachnaya-East kimberlite magma as the measured H2O abundances are particular low (<0.5 wt%). Instead, we are in position to draw analogy with the Oldoinyo Lengai natrocarbonatite magma, given the observed similarities in temperature (Kamenetsky et al., 2004) and composition. At low eruption temperature (< 600$^{o}$C) the natrocarbonatite magma has exceptionally low density (2170 kg/m$^3$ ; Dawson et al. (1996), viscosity (0.1-5 Pa s ; Dawson et al., 1996; Keller & Krafft, 1990; Norton & Pinkerton, 1997) and fast flow velocities (1-5 m/s ; Keller & Krafft, 1990). The effect of halogens on reducing apparent viscosity of the carbonatite magma (three orders of magnitude for a three-fold increase in halogen content; Norton & Pinkerton, 1997) makes us confident that enrichment of the Udachnaya-East kimberlite in chlorine (at least 3 wt%) is a key chemical factor responsible for unique rheological properties of kimberlite magmas.

### 7.5 Implications from kimberlites and carbonatites worldwide

The enrichment of the Udachnaya-East kimberlite in alkali carbonates and chlorides, if a primary mantle-derived signature, could have been present in other group-I kimberlites

prior to obliteration by common pervasive alteration. Study of melt inclusions trapped in magmatic phenocrysts during crystallisation allows seeing compositions beyond effects of postmagmatic modifications. The study of other least altered kimberlites emplaced into magmatic or metamorphic rocks in the terranes containing little or no sedimentary cover, namely the Gahcho Kué, Jericho, Aaron and Leslie pipes in the Slave Craton (Canada) and the Majuagaa dyke in southern West Greenland, helped to further enhanced the significance of the carbonate-chloride melt composition (Kamenetsky et al., 2009b).

The study of olivine and olivine-hosted melt inclusions in partially altered kimberlites from Canada and Greenland (Kamenetsky et al., 2009b), aimed at comparison with the fresh Udachnaya-East kimberlite and followed by implications of sodium- and chlorine-rich compositions of the parental kimberlite melt, has a precedent in the history of petrological and mineralogical studies of carbonatites. Unlike all ancient intrusive and extrusive carbonatite rocks composed of calcite and/or dolomite, the presently erupting carbonatitic magmas of the Oldoinyo Lengai volcano in Tanzania provides evidence for alkali- and halogen-rich anhydrous melts forming carbonatites. Following the discovery of these natrocarbonatite lavas (Dawson, 1962b) and building on the ideas of von Eckermann (1948), the primary/parental nature of such compositions was defended in a number of empirical (e.g., Clarke & Roberts, 1986; Dawson et al., 1987; Deans & Roberts, 1984; Gittins & McKie, 1980; Hay, 1983; Keller & Zaitsev, 2006; Le Bas, 1987; Schultz et al., 2004; Turner, 1988) and experimental (Safonov et al., 2007; Wallace & Green, 1988) studies. A strong support for the role of alkalies and halogens in magmas parental to mafic silicate intrusions and related carbonatites is further provided by melt/fluid inclusion research (e.g., Andreeva et al., 2006; Aspden, 1980; Aspden, 1981; Kogarko et al., 1991; Le Bas, 1981; Le Bas & Aspden, 1981; Panina, 2005; Panina & Motorina, 2008; Veksler et al., 1998). Syn- and postmagmatic release of alkalies from carbonatite magmas and rocks is recorded respectively in alkaline (mainly soda-dominant) metasomatic "fenitisation halos" around intrusive carbonatite bodies (e.g., (Bailey, 1993; Buhn & Rankin, 1999; Le Bas, 1987; McKie, 1966; Morogan & Lindblom, 1995) and references therein) and rapid decomposition of alkali- and chlorine-bearing minerals in the natrocarbonatites (Dawson, 1962b; Genge et al., 2001; Keller & Zaitsev, 2006; Mitchell, 2006). Same processes can be applicable to kimberlitic magmas in general, during and after their emplacement, as recorded in fenitisation of country rocks (Masun et al., 2004; Smith et al., 2004 and references therein) and gradation from Na-rich "deep" to Na-poor "shallow" kimberlite in the Udachnaya-East pipe.

The groundmass of most kimberlites, including altered kimberlites from the Udachnaya pipe, contain no alkali carbonates and chlorides and have very little $Na_2O$ (<0.2 wt%). We believe that alteration disturbs original melt compositions, with the alkaline elements and chlorine being mostly affected. However, the compositions of melt inclusions and Cl-rich serpentine are indicative of the chemical signature of a melt in which olivine crystallised and accumulated. It appears that enrichment in alkalies and chlorine, as seen in unaltered Udachnaya-East kimberlites, has been significant in other kimberlites prior to their alteration, and thus can be assigned deep mantle origin.

### 7.6 Two populations of olivine in kimberlites: Fellow-travellers or close relatives?

Our work on the uniquely unaltered Udachnaya-East kimberlite concurs with what has been shown in other mineralogical studies of other kimberlites, namely, the presence of morphologically distinct populations of olivine. One population is represented by large

rounded grains (olivine-I of disputed origin), whereas another type of olivine is typically smaller but better shaped crystals (olivine-II or groundmass phenocrysts). It has been advocated in the literature that olivine may provide valuable clues to processes of kimberlite formation, transport and emplacement (e.g. Boyd & Clement, 1977; Mitchell, 1973; Mitchell, 1986; Moore, 1988; Skinner, 1989).

Mitchell & Tappe (2010), Mitchell (1973; 1986), and Moore (1988) considered olivine from both populations to be phenocrysts (cognate phenocrysts of olivine-I from high-pressure crystallisation of the kimberlite melt, and groundmass olivine-II), although up to 40 % of olivine was assigned to xenocrystic origin from various mantle and lithospheric sources. A similar conclusion can be endorsed by the extreme diversity of peridotite xenoliths within the Udachnaya-East kimberlite (Shimizu et al., 1997; Sobolev, 1977; Sobolev et al., 2009). The absence of primary melt inclusions and presence of Cr-diopside inclusions in olivine-I also argue against their phenocrystic origin.

Xenocrystic origin of some or all grains of olivine-I does not preclude this olivine being overgrown by the "phenocrystic" olivine. Both types of olivine are transported together, and thus all changes related to chemical and mechanical resorption should be equally imposed on them, making a morphological distinction subjective. Both olivine populations in the studied Udachnaya-East samples demonstrate striking compositional similarity in their Fo values (Fig. 6) and oxygen isotope values (Kamenetsky et al., 2008). Trace elements abundances are also indistinguishable for the olivine-I and core sections of the groundmass olivine (Fig. 6). Moreover, in many cases the olivine-II cores have original crystal faces ground away (Fig. 7), and thus their shapes are similar to those of round olivine-I. It is most likely that crystals that now show as relics in the olivine-II cores were formed at depth and transported upwards in a crystal mush.

Morphological and chemical resemblance between olivine-I and cores of olivine-II can be related to similar chemical and physical conditions exerted during olivine growth (or re-crystallisation) and transport to the surface. If both olivine populations are related, their common origin might be tracked down to the earliest and deepest stages of the kimberlite evolutionary story, i.e. when and where primary (protokimberlite) magma derived and started ascent.

### 7.7 Evolutionary storyline of the kimberlite parental melt

The Udachnaya-East groundmass olivine has a clear compositional structure, where the cores with variable Fo values can be distinguished from the rims with limited range in Fo values (Fig. 6b). It should be emphasised again that the olivine-II rims are essentially uniform with respect to major elements, but minor elements fluctuate strongly, especially Ni abundances which reach maximum near the core-rim boundary, then decrease rapidly towards the outer rims (Fig. 6b). Broadly similar compositional features, namely two groups of olivine with normal and reversed core to rim zonation and similar ranges in Fo and trace element contents, have been previously described in the groundmass olivine in other kimberlites, diamondiferous and barren (Fedortchouk & Canil, 2004; Moore, 1988; Skinner, 1989).

Although the origin of olivine cores (cognate vs exotic) is still debatable, the overall compositional analogy between groundmass olivine from different pipes and different kimberlite provinces argue for that 1) origin of cores and rims of groundmass olivine are intimately linked to kimberlite genesis and evolution; 2) in each case physical and chemical

conditions of olivine formation are closely similar; 3) olivine cores and rims originate in different conditions; and 4) variable Fo compositions of cores reflect varying sources or changing conditions, whereas similar Fo values of rims reflect major buffering event.

Composition and zoning of the Udachnaya-East olivine-II are not unique; similar principle compositional characteristics of groundmass olivine phenocrysts (variable and constant Fo of cores and rims, respectively, and variable trace elements at a given Fo of the olivine rims; Fig. 6b) are described in a number of kimberlite suites (e.g., Boyd & Clement, 1977; Emeleus & Andrews, 1975; Fedortchouk & Canil, 2004; Hunter & Taylor, 1984; Kirkley et al., 1989; Mitchell, 1978; Mitchell, 1986; Moore, 1988; Nielsen & Jensen, 2005; Skinner, 1989). Compared to the ambiguous origin of the olivine cores, the rims of olivine-II most certainly crystallised from a melt transporting these crystals to the surface. This is best supported by the cases where several cores of different size, shape and composition are enclosed within a single olivine-II grain (Fig. 7 g, h). As indicated by mineral inclusions, the olivine-II rims formed together with phlogopite, perovskite, minerals of spinel group, rutile and orthopyroxene, i.e. common groundmass minerals (except orthopyroxene) from a melt that is present as melt inclusions in the olivine rims and healed fractures in the olivine-II cores and olivine-I (Fig. 3, 8).

Numerous studies indicate that most common xenoliths in kimberlites are garnet lherzolites, but surprisingly low abundance of orthopyroxene among xenocrysts and macrocrysts has been intriguing (Mitchell, 1973; Mitchell, 2008; Patterson et al., 2009; Skinner, 1989). Low silica activity in the kimberlite magma was offered as an explanation for instability of orthopyroxene, especially at sub-surface pressures (Mitchell, 1973). On the other hand, crystallising groundmass olivine rims and the presence of orthopyroxene inclusions in this olivine (Kamenetsky et al., 2008; Kamenetsky et al., 2009a) seem to be inconsistent with each other. One explanation is that orthopyroxene inclusions (often in groups and always associated with $CO_2$ bubbles) can result from the local reaction of olivine with $CO_2$ fluid ($2SiO_4^{-4} + 2CO_2 \rightarrow Si_2O_6^{-4} + 2CO_3^{-2}$).

A limited range of Fo content in the olivine-II rims, but variable trace element abundances (Fig. 6b) suggest crystallisation over a small temperature range or/and buffering of the magma at a constant Fe/Mg with fractionating Ni, Mn and Ca. In many instances, where the cores are seemingly affected by diffusion (Fig. 7 b, c, f, h) and have a surrounding layer of distinct composition (Fig. 7 a, e, h), the uniform Fo in the rims can reflect attempts by the crystals to equilibrate with a final hybrid magma (Mitchell, 1986). We also propose that the buffering of Fe/Mg can occur if the Mg–Fe distribution coefficient (Kd) between olivine and a carbonate-rich kimberlite melt is significantly higher than for common basaltic systems (i.e. 0.3±0.03). This reflects significantly smaller Mg-Fe fractionation between silicates and carbonate melt, possibly as a result of complexing between carbonate and $Mg^{2+}$ ions (Green & Wallace, 1988; Moore, 1988). The implied higher Kd for carbonatitic liquids, and especially Ca-rich carbonate, has been supported by experimental evidence (Dalton & Wood, 1993; Girnis et al., 2005). Probably an increase in Kd is even more pronounced for alkali-rich carbonatitic liquids.

The melt crystallising the rims of the Udachnaya-East groundmass olivine is represented by the carbonate-chloride matrix of the rocks (Kamenetsky et al., 2004; Kamenetsky et al., 2007a), and by the melt inclusions in olivine (Fig. 3, 8). The composition of this melt is unusually enriched in alkali carbonates and chlorides, but low in aluminosilicate components (Kamenetsky et al., 2004; Kamenetsky et al., 2007a). The crystallisation of

olivine from this melt implies saturation in the olivine component, which makes this melt different from the alkali carbonate melt experimentally produced at mantle P-T conditions and low melting extents (Sweeney et al., 1995; Wallace & Green, 1988). How and where is the saturation in olivine acquired?

Study of the olivine populations and complex zoning of the groundmass olivine in the Udachnaya-East and other kimberlites (Kamenetsky et al., 2008; Kamenetsky et al., 2009b) provides evidence that olivine crystals were first entrapped by the melt at depth, then partly abraded, dissolved and recrystallised on ascent, and finally regenerated during emplacement. We suggest that the history of kimberlitic olivine is owed to the extraordinary melt composition, as well as conditions during melt generation and emplacement. In our scenario, a key role is played by the chloride-carbonate (presumably protokimberlite) melt, which forces strong mechanical abrasion and dissolution of the silicate minerals from country rocks in the mantle and lithosphere. Such a melt is capable of accumulating Si and Mg, but only to a certain limit, above which an immiscible Cl-bearing carbonate-silicate liquid appears (Safonov et al., 2007). The amount of forsterite that can be dissolved in the sodium carbonate liquid at 10 kbar and 1300°C is found to be 16 wt% (Hammouda & Laporte, 2000). Dissolution of olivine and other silicate phases at high pressure does not proceed beyond the saturation, and is closely followed by precipitation of olivine (Hammouda & Laporte, 2000). Therefore, ascending kimberlite magma, although being more Si-rich than its parental melt and loaded with xenocrysts and xenoliths, remains buoyant enough to continue rapid ascent. At emplacement, the magma releases the dissolved silicate component in the form of groundmass olivine rims and minor silicate minerals, thus driving the residual melt towards original chloride-carbonate compositions (Kamenetsky et al., 2007a).

## 8. Concluding remarks

Dry, chlorine-bearing alkali minerals in the Udachnaya-East kimberlite are products of crystallisation of the mantle-derived, uncontaminated melt. We suggest that a composition rich in alkalies, $CO_2$ and Cl may be a viable alternative to the currently favoured ultramafic kimberlite magma. A "salty" kimberlite composition can explain trace element signatures consistent with low degrees of partial melting, low temperatures of crystallisation and exceptional rheological properties responsible for fast ascent and the magma's ability to carry abundant high-density mantle nodules and crystals. Evidence for these components, notably Cl and alkalies, is only preserved in an ultrafresh kimberlite such as Udachnaya-East. Nevertheless, Cl-bearing minerals of the type reported here have also been found in the groundmass and melt inclusions in kimberlites from Canada and Greenland (Kamenetsky et al., 2009b). The possible existence of chloride–carbonate liquids within the diamond stability field can be inferred from experiments in the model silicate system with addition of Na-Ca carbonate and K-chloride (Safonov et al., 2010; Safonov et al., 2007; Safonov et al., 2009). These experiments also show that Cl-bearing carbonate-silicate and Si-bearing chloride-carbonate melts evolve towards Cl-rich carbonatitic liquids with decreasing temperature, providing a possible explanation for chlorine- and alkali-enriched microinclusions in some diamonds from Udachnaya-East (Zedgenizov & Ragozin, 2007) and other kimberlites in South Africa and Canada (Izraeli et al., 2001; Klein-BenDavid et al., 2007; Tomlinson et al., 2006). Brine inclusions in diamonds from various kimberlites, and the inferred role of chlorides in diamond nucleation and growth (Palyanov et al., 2007;

Tomlinson et al., 2004) further illustrate the potential significance of mantle-derived "salty" fluids sampled by the kimberlite melt and fortuitously preserved at Udachnaya-East.

## 9. Acknowledgments

We are indebted to Victor Sharygin, Alexander Golovin and Nikolai Pokhilenko who collected and supplied kimberlite samples for these studies and co-authored previous publications. Alexander Sobolev initiated and supervised PhD studies of Maya Kamenetsky and contributed a wealth of provocative ideas for discussion. We thank D. Kuzmin, P. Robinson, S. Gilbert, K. McGoldrick, K. Gőmann, and L. Danyushevsky for providing help with different analyses. The results and ideas were discussed with many researchers at different conferences. In particular, we are grateful to D.H. Green, B. Dawson, G. Brey, C. Ballhaus, G. Yaxley, R. Mitchell, O. Navon, N. Sobolev, O. Safonov, A. Chakhmouradian, S. Kostrovitsky, S. Tappe, S. Matveev, M. Kopylova, L. Heaman, Ya. Fedortchouk and I. Veksler for advice, moral support and friendly criticism. This study was initially (2003-2005) supported by the Alexander von Humboldt Foundation (Germany) in the form of the Wolfgang Paul Award to A. Sobolev and the Friedrich Wilhelm Bessel Award to V. Kamenetsky. Financial support for these studies in 2005-2009 was provided by an Australian Research Council Professorial Fellowship and Discovery Grant to V. Kamenetsky "Unmixing in Magmas: Melt and Fluid Inclusion Constraints on Identity, Timing, and Evolution of Immiscible Fluids, Salt and Sulphide Melts ".

## 10. References

Andreeva, I.A., Kovalenko, V.I., Kononkova, N.N., (2006) Natrocarbonatitic melts of the Bol'shaya Tagna Massif, the eastern Sayan region. *Doklady Earth Sciences*, 408(4), 542-546.

Arndt, N.T., Guitreau, M., Boullier, A.M., Le Roex, A., Tommasi, A., Cordier, P., Sobolev, A., (2010) Olivine, and the origin of kimberlite. *Journal of Petrology*, 51(3), 573-602.

Aspden, J.A., (1980) The mineralogy of primary inclusions in apatite crystals extracted from Alno ijolite. *Lithos*, 13(3), 263-268.

Aspden, J.A., (1981) The composition of solid inclusions and the occurrence of shortite in apatites from the Tororo carbonatite complex of Eastern Uganda. *Mineralogical Magazine*, 44(334), 201-204.

Bailey, D.K., (1993) Carbonate magmas. *Journal of the Geological Society, London*, 150, 637-651.

Boyd, F.R., Clement, C.R., (1977) Compositional zoning of olivines in kimberlites from the De Beers mine, Kimberley, South Africa. *Carnegie Institution of Washington Yearbook*, 76, 485-493.

Brasier, M.D., Sukhov, S.S., (1998) The falling amplitude of carbon isotopic oscillations through the lower to middle Cambrian: northern Siberia data. *Canadian Journal of Earth Sciences*, 35(4), 353-373.

Brett, R.C., Russell, J.K., Moss, S., (2009) Origin of olivine in kimberlite: Phenocryst or impostor? *Lithos*, 112, 201-212.

Buhn, B., Rankin, A.H., (1999) Composition of natural, volatile-rich Na-Ca-REE-Sr carbonatitic fluids trapped in fluid inclusions. *Geochimica et Cosmochimica Acta*, 63(22), 3781-3797.

Bulanova, G.P., Griffin, W.J., Ryan, C.G., (1998) Nucleation environment of diamonds from Yakutian kimberlites. *Mineralogical Magazine*, 62, 409-419.

Burgess, R., Turner, G., Harris, J.W., (1992) $^{40}$Ar-$^{39}$Ar laser probe studies of clinopyroxene inclusions in eclogitic diamonds. *Geochimica et Cosmochimica Acta*, 56(1), 389-402.

Canil, D., Fedortchouk, Y., (1999) Garnet dissolution and the emplacement of kimberlites. *Earth and Planetary Science Letters*, 167(3-4), 227-237.

Carroll, M.R., Webster, J.D., (1994) Solubilities of sulfur, noble gases, nitrogen, chlorine, and fluorine in magmas. In: M.R. Carroll, J.R. Holloway (Eds.), *Volatiles in magmas. Reviews in mineralogy, 30* (Ed. by M.R. Carroll, J.R. Holloway), pp. 231-279. Mineralogical Society of America, Washington.

Chakhmouradian, A.R., Mitchell, R.H., (2000) Occurrence, alteration patterns and compositional variation of perovskite in kimberlites. *Canadian Mineralogist*, 38, 975-994.

Clarke, M.G.C., Roberts, B., (1986) Carbonated melilitites and calcitized alkalicarbonatites from Homa Mountain, western Kenya: a reinterpretation. *Geological Magazine*, 123, 683-692.

Clement, C.R., Skinner, E.M.W., (1985) A textural-genetic classification of kimberlites. *Transactions of Geological Society of South Africa*, 88, 403-409.

Clement, C.R., Skinner, E.M.W., Scott Smith, B.H., (1984) Kimberlite re-defined. *Journal of Geology*, 32, 223-228.

Cooper, A.F., Gittins, J., Tuttle, O.F., (1975) The system $Na_2CO_3$-$K_2CO_3$-$CaCO_3$ at 1 kilobar and its significance in carbonatite petrogenesis. *American Journal of Science*, 275, 534-560.

Dalton, J.A., Wood, B.J., (1993) The compositions of primary carbonate melts and their evolution through wallrock reaction in the mantle. *Earth and Planetary Science Letters*, 119(4), 511-525.

Dawson, J.B., (1962a) The geology of Oldoinyo Lengai. *Bulletin Volcanologique*, 24, 349-387.

Dawson, J.B., (1962b) Sodium carbonate lavas from Oldoinyo Lengai, Tanganyika. *Nature*, 195(4846), 1075-1076.

Dawson, J.B., (1980) *Kimberlites and their xenoliths*. Springer-Verlag, Berlin.

Dawson, J.B., (1989) Sodium carbonatite extrusions from Oldoinyo Lengai, Tanzania: implications for carbonatite complex genesis. In: K. Bell (Ed.), *Carbonatites. Genesis and evolution* (Ed. by K. Bell), pp. 255-277. Unwin Hyman, London.

Dawson, J.B., Garson, M.S., Roberts, B., (1987) Altered former alkalic carbonatite lava from Oldoinyo Lengai, Tanzania: Inferences for calcite carbonatite lavas. *Geology*, 15(8), 765-768.

Dawson, J.B., Hawthorne, J.B., (1973) Magmatic sedimentation and carbonatitic differentiation in kimberlite sills at Benfontein, South Africa. *Journal of the Geological Society of London*, 129(1), 61-85.

Dawson, J.B., Pinkerton, H., Norton, G.E., Pyle, D.M., (1990) Physicochemical properties of alkali carbonatite lavas: Data from the 1988 eruption of Oldoinyo Lengai, Tanzania. *Geology*, 18(3), 260-263.

Dawson, J.B., Pyle, D.M., Pinkerton, H., (1996) Evolution of natrocarbonatite from a wollastonite nephelinite parent: Evidence from the June, 1993 eruption of Oldoinyo Lengai, Tanzania. *Journal of Geology*, 104(1), 41-54.

Deans, T., Roberts, B., (1984) Carbonatite tuffs and lava clasts of the Tinderet foothills, western Kenya: a study of calcified natrocarbonatites. *Journal of the Geological Society, London*, 141(MAY), 563-580.

Edgar, A.D., Arima, M., Baldwin, D.K., Bell, D.R., Shee, S.R., Skinner, E.M.W., Walker, E.C., (1988) High-pressure-high-temperature melting experiments on a $SiO_2$-poor aphanitic kimberlite from the Wesselton mine, Kimberley, South Africa. *American Mineralogist*, 73(5-6), 524-533.

Edgar, A.D., Charbonneau, H.E., (1993) Melting experiments on a $SiO_2$-poor, CaO-rich aphanitic kimberlite from 5-10 GPa and their bearing on sources of kimberlite magmas. *American Mineralogist*, 78(1-2), 132-142.

Eggler, D.H., (1989) Kimberlites: how do they form? In: J. Ross, et al. (Ed.), *Kimberlites and related rocks: their composition, occurrence, origin and emplacement*, *1* (Ed. by J. Ross, et al.), pp. 489-504. Blackwell Scientific Publications, Sydney.

Emeleus, C.H., Andrews, J.R., (1975) Mineralogy and petrology of kimberlite dyke and sheet intrusions and included peridotite xenoliths from South West Greenland. *Physics and Chemistry of the Earth*, 9, 179-198.

Fedortchouk, Y., Canil, D., (2004) Intensive variables in kimberlite magmas, Lac de Gras, Canada and implications for diamond survival. *Journal of Petrology*, 45(9), 1725-1745.

Francis, D., Patterson, M., (2009) Kimberlites and aillikites as probes of the continental lithospheric mantle. *Lithos*, 109(1-2), 72-80.

Fraser, K.J., Hawkesworth, C.J., Erlank, A.J., Mitchel, R.H., Scott-Smith, B.H., (1985) Sr, Nd, and Pb isotope and minor element geochemistry of lamproites and kimberlites. *Earth and Planetary Science Letters*, 76, 57-70.

Fulignati, P., Kamenetsky, V.S., Marianelli, P., Sbrana, A., Mernagh, T.P., (2001) Melt inclusion record of immiscibility between silicate, hydrosaline and carbonate melts: Applications to skarn genesis at Mount Vesuvius. *Geology*, 29(11), 1043-1046.

Genge, M.J., Balme, M., Jones, A.P., (2001) Salt-bearing fumarole deposits in the summit crater of Oldoinyo Lengai, Northern Tanzania: interactions between natrocarbonatite lava and meteoric water. *Journal of Volcanology and Geothermal Research*, 106(1-2), 111-122.

Girnis, A.V., Bulatov, V.K., Brey, G.P., (2005) Transition from kimberlite to carbonatite melt under mantle parameters: An experimental study. *Petrology*, 13(1), 1-15.

Girnis, A.V., Ryabchikov, I.D., (2005) Conditions and mechanisms of generation of kimberlite magmas. *Geology of Ore Deposits*, 47(6), 476–487.

Gittins, J., (1989) The origin and evolution of carbonatite magmas. In: K. Bell (Ed.), *Carbonatites. Genesis and evolution* (Ed. by K. Bell), pp. 580-599. Unwin Hyman, London.

Gittins, J., McKie, D., (1980) Alkalic carbonatite magmas: Oldoinyo Lengai and its wider applicability. *Lithos*, 13, 213-215.

Golovin, A.V., Sharygin, V.V., Pokhilenko, N.P., (2007) Melt inclusions in olivine phenocrysts in unaltered kimberlites from the Udachnaya-East pipe, Yakutia: Some aspects of kimberlite magma evolution during late crystallization stages. *Petrology*, 15(2), 168-183.

Golovin, A.V., Sharygin, V.V., Pokhilenko, N.P., Mal'kovets, V.G., Kolesov, B.A., Sobolev, N.V., (2003) Secondary melt inclusions in olivine from unaltered kimberlites of the Udachnaya-East pipe, Yakutia. *Doklady Earth Sciences*, 388(1), 93-96.

Green, D.H., Wallace, M.E., (1988) Mantle metasomatism by ephemeral carbonatite melts. *Nature*, 336, 459-462.

Haggerty, S.E., (1999) A diamond trilogy: Superplumes, supercontinents, and supernovae. *Science*, 285, 851-860.

Hammouda, T., Laporte, D., (2000) Ultrafast mantle impregnation by carbonatite melts. *Geology*, 28(3), 283-285.

Hay, R.L., (1983) Natrocarbonatite tephra of Kerimasi volcano, Tanzania. *Geology*, 11(10), 599-602.

Heaman, L.M., (1989) The nature of the subcontinental mantle from Sr-Nd-Pb isotopic studies on kimberlitic perovskite. *Earth and Planetary Science Letters*, 92(3-4), 323-334.

Hunter, R.H., Taylor, L.A., (1984) Magma-mixing in the low velocity zone: kimberlitic megacrysts from Fayette County, Pennsylvania. *American Mineralogist*, 69, 16-29.

Izraeli, E.S., Harris, J.W., Navon, O., (2001) Brine inclusions in diamonds: a new upper mantle fluid. *Earth and Planetary Science Letters*, 187, 323-332.

Izraeli, E.S., Harris, J.W., Navon, O., (2004) Fluid and mineral inclusions in cloudy diamonds from Koffiefontein, South Africa. *Geochimica et Cosmochimica Acta*, 68, 2561-2575.

Jago, B.C., Gittins, J., (1991) The role of fluorine in carbonatite magma evolution. *Nature*, 349(6304), 56-58.

Kamenetsky, M.B., Sobolev, A.V., Kamenetsky, V.S., Maas, R., Danyushevsky, L.V., Thomas, R., Sobolev, N.V., Pokhilenko, N.P., (2004) Kimberlite melts rich in alkali chlorides and carbonates: a potent metasomatic agent in the mantle. *Geology*, 32(10), 845-848.

Kamenetsky, V.S., Kamenetsky, M.B., Sharygin, V.V., Faure, K., Golovin, A.V., (2007a) Chloride and carbonate immiscible liquids at the closure of the kimberlite magma evolution (Udachnaya-East kimberlite, Siberia). *Chemical Geology*, 237(3-4), 384-400.

Kamenetsky, V.S., Kamenetsky, M.B., Sharygin, V.V., Golovin, A.V., (2007b) Carbonate-chloride enrichment in fresh kimberlites of the Udachnaya-East pipe, Siberia: A clue to physical properties of kimberlite magmas? *Geophysical Research Letters*, 34(9), L09316, doi:10.1029/2007GL029389.

Kamenetsky, V.S., Kamenetsky, M.B., Sobolev, A.V., Golovin, A.V., Demouchy, S., Faure, K., Sharygin, V.V., Kuzmin, D.V., (2008) Olivine in the Udachnaya-East kimberlite (Yakutia, Russia): types, compositions and origins. *Journal of Petrology*, 49(4), 823-839.

Kamenetsky, V.S., Kamenetsky, M.B., Sobolev, A.V., Golovin, A.V., Sharygin, V.V., Pokhilenko, N.P., Sobolev, N.V., (2009a) Can pyroxenes be liquidus minerals in the kimberlite magma? *Lithos*, 112, 213-222.

Kamenetsky, V.S., Kamenetsky, M.B., Weiss, Y., Navon, O., Nielsen, T.F.D., Mernagh, T.P., (2009b) How unique is the Udachnaya-East kimberlite? Comparison with kimberlites from the Slave Craton (Canada) and SW Greenland. *Lithos*, 112, 334-346.

Kamenetsky, V.S., Maas, R., Kamenetsky, M.B., Paton, C., Phillips, D., Golovin, A.V., Gornova, M.A., (2009c) Chlorine from the mantle: Magmatic halides in the Udachnaya-East kimberlite, Siberia. *Earth and Planetary Science Letters*, 285(1-2), 96-104.

Keller, J., Krafft, M., (1990) Effusive natrocarbonatite activity of Oldoinyo Lengai, June 1988. *Bulletin of Volcanology*, 52(8), 629-645.

Keller, J., Spettel, B., (1995) The trace element compositions and petrogenesis of natrocarbonatites. In: K. Bell, J. Keller (Eds.), *Carbonatite volcanism: Oldoinyo Lengai and petrogenesis of natrocarbonatites* (Ed. by K. Bell, J. Keller), pp. 70-86. Springer-Verlag.

Keller, J., Zaitsev, A.N., (2006) Calciocarbonatite dykes at Oldoinyo Lengai, Tanzania: The fate of natrocarbonatite. *Canadian Mineralogist*, 44, 857-876.

Kelley, S.P., Wartho, J.A., (2000) Rapid kimberlite ascent and the significance of Ar-Ar ages in xenolith phlogopites. *Science*, 289(5479), 609-611.

Kinny, P.D., Griffin, W.L., Heaman, L.M., Brakhfogel, F.F., Spetsius, Z.V., (1997) SHRIMP U-Pb ages of perovskite from Yakutian kimberlites. *Russian Geology and Geophysics*, 38(1), 91-99.

Kirkley, M.B., Smith, H.S., Gurney, J.J., (1989) Kimberlite carbonates - a carbon and oxygen stable isotope study. In: J. Ross, et al. (Ed.), *Kimberlites and related rocks: their composition, occurrence, origin and emplacement*, *1* (Ed. by J. Ross, et al.), pp. 264-281. Blackwell Scientific Publications, Sydney.

Kjarsgaard, B.A., Pearson, D.G., Tappe, S., Nowell, G.M., Dowall, D.P., (2009) Geochemistry of hypabyssal kimberlites from Lac de Gras, Canada: Comparisons to a global database and applications to the parent magma problem. *Lithos*, 112, 236-248.

Klein-BenDavid, O., Izraeli, E.S., Hauri, E., Navon, O., (2007) Fluid inclusions in diamonds from the Diavik mine, Canada and the evolution of diamond-forming fluids. *Geochimica Et Cosmochimica Acta*, 71(3), 723-744.

Klein-BenDavid, O., Izraeli, E.S., Hauri, E.H., Navon, O., (2004) Mantle fluid evolution - a tale of one diamond. *Lithos*, 77(1-4), 243-253.

Kogarko, L.N., Plant, D.A., Henderson, C.M.B., Kjarsgaard, B.A., (1991) Na-rich carbonate inclusions in perovskite and calzirtite from the Guli Intrusive Ca-carbonatite, Polar Siberia. *Contributions to Mineralogy and Petrology*, 109(1), 124-129.

Kopylova, M.G., Matveev, S., Raudsepp, M., (2007) Searching for parental kimberlite melt. *Geochimica et Cosmochimica Acta*, 71, 3616–3629.

Kostrovitsky, S.I., Morikiyo, T., Serov, I.V., Yakovlev, D.A., Amirzhanov, A.A., (2007) Isotope-geochemical systematics of kimberlites and related rocks from the Siberian Platform. *Russian Geology and Geophysics*, 48(3), 272-290.

Krafft, M., Keller, J., (1989) Temperature measurements in carbonatite lava lakes and flows from Oldoinyo Lengai, Tanzania. *Science*, 245(4914), 168-170.

Le Bas, M.J., (1981) Carbonatite Magmas. *Mineralogical Magazine*, 44(334), 133-140.

Le Bas, M.J., (1987) Nephelinites and carbonatites. In: J.G. Fitton, B.G.J. Upton (Eds.), *Alkaline igneous rocks*, *Special Publication 30* (Ed. by J.G. Fitton, B.G.J. Upton), pp. 53-83. Geological Society of London.

Le Bas, M.J., Aspden, J.A., (1981) The comparability of carbonatitic fluid inclusions in ijolites with natrocarbonatite lava. *Bulletin of Volcanology*, 44, 429-438.

le Roex, A.P., Bell, D.R., Davis, P., (2003) Petrogenesis of group I kimberlites from Kimberley, South Africa: evidence from bulk-rock geochemistry. *Journal of Petrology*, 44(12), 2261-2286.

Maas, R., Kamenetsky, M.B., Sobolev, A.V., Kamenetsky, V.S., Sobolev, N.V., (2005) Sr, Nd, and Pb isotope evidence for a mantle origin of alkali chlorides and carbonates in the Udachnaya kimberlite, Siberia. *Geology*, 33(7), 549–552.

Marshintsev, V.K., (1986) *Vertical heterogeneity of kimberlite bodies in Yakutiya*. Nauka, Novosibirsk.

Marshintsev, V.K., Migalkin, K.N., Nikolaev, N.C., Barashkov, Y.P., (1976) Unaltered kimberlite of the Udachnaya East pipe. *Transactions (Doklady) of the USSR Academy of Sciences*, 231, 961-964.

Maslovskaja, M.N., Yegorov, K.N., Kolosnitsyna, T.I., Brandt, S.B., (1983) Strontium isotope composition, Rb-Sr absolute age, and rare alkalies in micas from Yakutian kimberlites. *Doklady Akademii Nauk SSSR*, 266(2), 451-455.

Masun, K.M., Doyle, B.J., Ball, S., Walker, S., (2004) The geology and mineralogy of the Anuri kimberlite, Nunavut, Canada. *Lithos*, 76(1-4), 75-97.

McKie, D., (1966) Fenitization. In: O.F. Tuttle, J. Gittins (Eds.), *Carbonatites* (Ed. by O.F. Tuttle, J. Gittins), pp. 261-294. John Wiley and Sons, London.

Mitchell, R., Tappe, S., (2010) Discussion of "Kimberlites and aillikites as probes of the continental lithospheric mantle", by D. Francis and M. Patterson (Lithos v. 109, p. 72-80). *Lithos*, 115(1-4), 288-292.

Mitchell, R.H., (1973) Composition of olivine, silica activity and oxygen fugacity in kimberlite. *Lithos*, 6, 65-81.

Mitchell, R.H., (1978) Mineralogy of the Elwin Bay kimberlite, Somerset Island, N.W.T., Canada. *American Mineralogist*, 63, 47-57.

Mitchell, R.H., (1986) *Kimberlites: mineralogy, geochemistry and petrology*. Plenum Press, New York.

Mitchell, R.H., (1989) Aspects of the petrology of kimberlites and lamproites: some definitions and distinctions. In: J. Ross, et al. (Ed.), *Kimberlites and related rocks: their composition, occurrence, origin and emplacement*, *1* (Ed. by J. Ross, et al.), pp. 7-45. Blackwell Scientific Publications, Sydney.

Mitchell, R.H., (1995) *Kimberlites, orangeites and related rocks*. Plenium Press, New York.

Mitchell, R.H., (2006) An ephemeral pentasodium phosphate carbonate from natrocarbonatite lapilli, Oldoinyo Lengai, Tanzania. *Mineralogical Magazine*, 70(2), 211-218.

Mitchell, R.H., (2008) Petrology of hypabyssal kimberlites: Relevance to primary magma compositions,. *Journal of Volcanology and Geothermal Research*, 174, 1-8.

Moore, A.E., (1988) Olivine: a monitor of magma evolutionary paths in kimberlites and olivine melilitites. *Contributions to Mineralogy and Petrology*, 99, 238-248.

Morogan, V., Lindblom, S., (1995) Volatiles associated with the alkaline - carbonatite magmatism at Alno, Sweden: A study of fluid and solid inclusions in minerals from the Langarsholmen ring complex. *Contributions to Mineralogy and Petrology*, 122(3), 262-274.

Nielsen, T.F.D., Jensen, S.M., (2005) The Majuagaa calcite-kimberlite dyke, Maniitsoq, southern West Greenland, pp. 59. Geological Survey of Denmark and Greenland, Report 2005/43.

Norton, G., Pinkerton, H., (1997) Rheological properties of natrocarbonatite lavas from Oldoinyo Lengai, Tanzania. *European Journal of Mineralogy*, 9(2), 351-364.

Nowell, G.M., Pearson, D.G., Bell, D.R., Carlson, R.W., Smith, C.B., Kempton, P.D., Noble, S.R., (2004) Hf isotope systematics of kimberlites and their megacrysts: New constraints on their source regions. *Journal of Petrology*, 45(8), 1583-1612.

Palyanov, Y.N., Shatsky, V.S., Sobolev, N.V., Sokol, A.G., (2007) The role of mantle ultrapotassic fluids in diamond formation. *Proceedings of the National Academy of Sciences of the United States of America*, 104(22), 9122-9127.

Pal'yanov, Y.N., Sokol, A.G., Borzdov, Y.M., Khokhryakov, A.F., (2002) Fluid-bearing alkaline carbonate melts as the medium for the formation of diamonds in the Earth's mantle: an experimental study. *Lithos*, 60, 145-159.

Panina, L.I., (2005) Multiphase carbonate-salt immiscibility in carbonatite melts: data on melt inclusions from the Krestovskiy massif minerals (Polar Siberia). *Contributions to Mineralogy and Petrology*, 150(1), 19-36.

Panina, L.I., Motorina, I.V., (2008) Liquid immiscibility in deeply derived magmas and the origin of carbonatite melts. *Geochemistry International*, 46(5), 448–464.

Pasteris, J.D., (1984) Kimberlites: Complex mantle melts. *Annual Review of Earth and Planetary Sciences*, 12, 133-153.

Paton, C., Hergt, J.M., Phillips, D., Woodhead, J.D., Shee, S.R., (2007) New insights into the genesis of Indian kimberlites from the Dharwar Craton via in situ Sr isotope analysis of groundmass perovskite. *Geology*, 35(11), 1011–1014.

Patterson, M., Francis, D., McCandless, T., (2009) Kimberlites: Magmas or mixtures? *Lithos*, 112, 191-200.

Pavlov, D.I., Ilupin, I.P., (1973) Halite in Yakutian kimberlite, its relation to serpentine and the source of its parent solutions. *Transactions (Doklady) of Russian Academy of Sciences*, 213(6), 178-180.

Pearson, D.G., Shirey, S.B., Carlson, R.W., Boyd, F.R., Pokhilenko, N.P., Shimizu, N., (1995) Re-Os, Sm-Nd, and Rb-Sr Isotope evidence for thick Archaean lithospheric mantle beneath the Siberian craton modified by multistage metasomatism. *Geochimica et Cosmochimica Acta*, 59(5), 959-977.

Price, S.E., Russell, J.K., Kopylova, M.G., (2000) Primitive magma from the Jericho Pipe, NWT, Canada: Constraints on primary kimberlite melt chemistry. *Journal of Petrology*, 41(6), 789-808.

Safonov, O.G., Kamenetsky, V.S., Perchuk, L.L., (2010) Carbonatite-to-kimberlite link in the chloride-carbonate-silicate systems: experimental approach and application to natural assemblages. *Journal of Petrology*, doi:10.1093/petrology/egq034.

Safonov, O.G., Perchuk, L.L., Litvin, Y.A., (2007) Melting relations in the chloride–carbonate–silicate systems at high-pressure and the model for formation of alkalic diamond–forming liquids in the upper mantle. *Earth and Planetary Science Letters*, 253, 112–128.

Safonov, O.G., Perchuk, L.L., Yapaskurt, V.O., Litvin, Y.A., (2009) Immiscibility of carbonate–silicate and chloride–carbonate melts in the kimberlite–$CaCO_3$–$Na_2CO_3$–KCl system at 4.8 GPa. *Doklady Earth Sciences*, 424(1), 142–146.

Schultz, F., Lehmann, B., Tawackoli, S., Rossling, R., Belyatsky, B., Dulski, P., (2004) Carbonatite diversity in the Central Andes: the Ayopaya alkaline province, Bolivia. *Contributions to Mineralogy and Petrology*, 148, 391-408.

Sharp, Z.D., Barnes, J.D., Brearley, A.J., Fischer, T., Chaussidon, M., Kamenetsky, V.S., (2007) Chlorine isotope homogeneity of the mantle, crust and carbonaceous chondrites. *Nature*, 446, 1062-1065.

Sharygin, V.V., Golovin, A.V., Pokhilenko, N.P., Sobolev, N.V., (2003) Djerfisherite in unaltered kimberlites of the Udachnaya-East pipe, Yakutia. *Doklady Earth Sciences*, 390(4), 554-557.

Shee, S.R., (1986) The petrogenesis of the Wesselton mine kimberlites, Kimberley, Cape Province, R.S.A. University of Cape Town.

Sheppard, S.M.F., Dawson, J.B., (1975) Hydrogen, carbon and oxygen isotope studies of megacryst and matrix minerals from Lesothan and South African kimberlites. *Physics and Chemistry of the Earth*, 9, 747-763.

Shimizu, N., Pokhilenko, N.P., Boyd, F.R., Pearson, D.G., (1997) Geochemical characteristics of mantle xenoliths from Udachnaya kimberlite pipe. *Russian Geology and Geophysics*, 38(1), 194-205.

Skinner, E.M.W., (1989) Contrasting Group I and Group II kimberlite petrology: towards a genetic model for kimberlites. In: J. Ross, et al. (Ed.), *Kimberlites and related rocks: their composition, occurrence, origin and emplacement*, *1* (Ed. by J. Ross, et al.), pp. 528-544. Blackwell Scientific Publications, Sydney.

Skinner, E.M.W., Clement, C.R., (1979) Mineralogical classification of Southern African kimberlites. In: F.R. Boyd, H.O.A. Meyer (Eds.), *Kimberlites, diatremes and diamonds: their geology, petrology and geochemistry* (Ed. by F.R. Boyd, H.O.A. Meyer), pp. 129-139. American Geophysical Union, Washington, D.C.

Smith, C.B., (1983) Pb, Sr and Nd isotopic evidence for sources of southern African Cretaceous kimberlites. *Nature*, 304, 51-54.

Smith, C.B., Gurney, J.J., Skinner, E.M.W., Clement, C.R., Ebrahim, N., (1985) Geochemical character of the southern African kimberlites: a new approach based on isotopic constraints. *Transactions of Geological Society of South Africa*, 88, 267-280.

Smith, C.B., Sims, K., Chimuka, L., Duffin, A., Beard, A.D., Townend, R., (2004) Kimberlite metasomatism at Murowa and Sese pipes, Zimbabwe. *Lithos*, 76(1-4), 219-232.

Sobolev, A.V., Sobolev, N.V., Smith, C.B., Dubessy, J., (1989) Fluid and melt compositions in lamproites and kimberlites based on the study of inclusions in olivine. In: J. Ross, et al. (Ed.), *Kimberlites and related rocks: their composition, occurrence, origin and emplacement*, *1* (Ed. by J. Ross, et al.), pp. 220-241. Blackwell Scientific Publications, Sydney.

Sobolev, N.V., (1977) *Deep-seated inclusions in kimberlites and the problem of the composition of the upper mantle*. American Geophysical Union, Washington, D.C.

Sobolev, N.V., Logvinova, A.M., Zedgenizov, D.A., Pokhilenko, N.P., Malygina, E.V., Kuzmin, D.V., Sobolev, A.V., (2009) Petrogenetic significance of minor elements in olivines from diamonds and peridotite xenoliths from kimberlites of Yakutia. *Lithos*, 112, 701-713.

Sparks, R.S.J., Baker, L., Brown, R.L., Field, M., Schumacher, J., Stripp, G., Walters, A., (2006) Dynamical constraints on kimberlite volcanism. *Journal of Volcanology and Geothermal Research*, 155, 18–48.

Spence, D.A., Turcotte, D.L., (1990) Buoyancy-driven magma fracture: A mechanism for ascent through the lithosphere and the emplacement of diamonds. *Journal of Geophysical Research*, 95(B4), 5133-5139.

Sun, S.-S., McDonough, W.F., (1989) Chemical and isotopic systematics of oceanic basalts: implications for mantle composition and processes. In: A.D. Saunders, M.J. Norry (Eds.), *Magmatism in the Ocean Basins*, *42* (Ed. by A.D. Saunders, M.J. Norry), pp. 313-345. Geological Society Special Publication, London.

Sweeney, R.J., Falloon, T.J., Green, D.H., (1995) Experimental constraints on the possible mantle origin of natrocarbonatite. In: K. Bell, J. Keller (Eds.), *Carbonatite volcanism: Oldoinyo Lengai and petrogenesis of natrocarbonatites*, *pdf* (Ed. by K. Bell, J. Keller), pp. 191-207. Springer-Verlag.

Tomlinson, E., Jones, A., Milledge, J., (2004) High-pressure experimental growth of diamond using C-$K_2CO_3$-KCl as an analogue for Cl-bearing carbonate fluid. *Lithos*, 77(1-4), 287-294.

Tomlinson, E.L., Jones, A.P., Harris, J.W., (2006) Co-existing fluid and silicate inclusions in mantle diamond. *Earth and Planetary Science Letters*, 250(3-4), 581-595.

Turner, D.C., (1988) Volcanic carbonatites of the Kaluwe complex, Zambia. *Journal of the Geological Society*, 145, 95-106.

Veksler, I.V., (2004) Liquid immiscibility and its role at the magmatic-hydrothermal transition: a summary of experimental studies. *Chemical Geology*, 210(1-4), 7-31.

Veksler, I.V., Nielsen, T.F.D., Sokolov, S.V., (1998) Mineralogy of crystallized melt inclusions from Gardiner and Kovdor ultramafic alkaline complexes: Implications for carbonatite genesis. *Journal of Petrology*, 39(11-12), 2015-2031.

von Eckermann, H., (1948) *The alkaline district of Alno Island*.

Wallace, M.E., Green, D.H., (1988) An experimental determination of primary carbonatite magma composition. *Nature*, 335(6188), 343-346.

Weis, D., Demaiffe, D., (1985) A depleted mantle source for kimberlites from Zaire: Nd, Sr and Pb isotopic evidence. *Earth and Planetary Science Letters*, 73, 269-277.

Zaitsev, A.N., Keller, J., (2006) Mineralogical and chemical transformation of Oldoinyo Lengai natrocarbonatites, Tanzania. *Lithos*, 91(1-4), 191-207.

Zedgenizov, D.A., Kagi, H., Shatsky, V.S., Sobolev, N.V., (2004) Carbonatitic melts in cuboid diamonds from Udachnaya kimberlite pipe (Yakutia): evidence from vibrational spectroscopy. *Mineralogical Magazine*, 68(1), 61-73.

Zedgenizov, D.A., Ragozin, A.L., (2007) Chloride-carbonate fluid in diamonds from the eclogite xenolith. *Doklady Earth Sciences*, 415(6), 961-964.

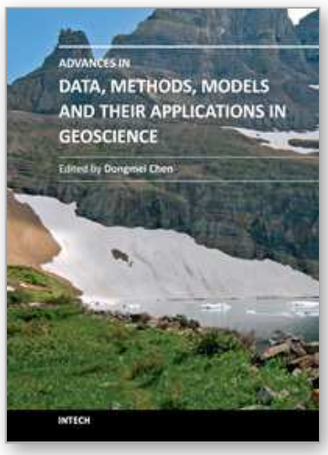


**Advances in Data, Methods, Models and Their Applications in Geoscience**

Edited by Dr. DongMei Chen

ISBN 978-953-307-737-6
Hard cover, 336 pages
**Publisher** InTech
**Published online** 22, December, 2011
**Published in print edition** December, 2011

With growing attention on global environmental and climate change, geoscience has experienced rapid change and development in the last three decades. Many new data, methods and modeling techniques have been developed and applied in various aspects of geoscience. The chapters collected in this book present an excellent profile of the current state of various data, analysis methods and modeling techniques, and demonstrate their applications from hydrology, geology and paleogeomorphology, to geophysics, environmental and climate change. The wide range methods and techniques covered in the book include information systems and technology, global position system (GPS), digital sediment core image analysis, fuzzy set theory for hydrology, spatial interpolation, spectral analysis of geophysical data, GIS-based hydrological models, high resolution geological models, 3D sedimentology, change detection from remote sensing, etc. Besides two comprehensive review articles, most chapters focus on in-depth studies of a particular method or technique.



**InTech Europe**
University Campus STeP Ri
Slavka Krautzeka 83/A
51000 Rijeka, Croatia
Phone: +385 (51) 770 447
Fax: +385 (51) 686 166
www.intechopen.com

**InTech China**
Unit 405, Office Block, Hotel Equatorial Shanghai
No.65, Yan An Road (West), Shanghai, 200040, China
中国上海市延安西路65号上海国际贵都大饭店办公楼405单元
Phone: +86-21-62489820
Fax: +86-21-62489821

IntechOpen